Friction

Review Article

Critical advances in superlubricity: From current challenges to sustainable development beyond laboratory

Huajie Tang[1], Wenli Deng[1], Jinjin Li[1], Jiaqi He[2], Xinchun Chen[1,✉]

Cite this article: Tang HJ, Deng WL, Li JJ, et al. *Friction* 2025, **13**(10): 9441075. https://doi.org/10.26599/FRICT.2025.9441075

ABSTRACT: Emerging superlubricity provides innovative scientific and engineering solutions for the sustainable future of human beings and nature. Although great progress has been made in the development of novel superlubricity systems and different mechanisms, considerable challenges remain before the engineering development of liquid superlubricity can be realized. Herein, the progress made towards achieving liquid superlubricity has been reviewed with emphasis on the current limitations, potential mechanisms, and future breakthroughs that will be expected to overcome these limitations. The perspectives are highlighted based on rigorous statistics and analyses according to the types of lubricants and materials of friction pairs. This review elucidates the key tribochemical mechanisms and research directions to break through the current limitations and provides constructive ideas for the engineering development of liquid superlubricity in the future, which will enable a sustainable future for human beings and nature.

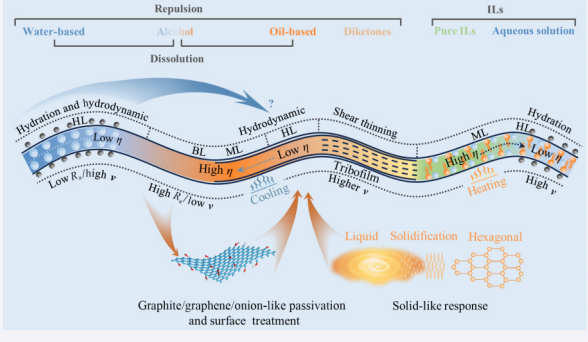

KEYWORDS: liquid superlubricity; ultralow friction; lubricants; tribology; wear

1 Introduction

Friction is the physical and chemical phenomenon of the relative motion of two objects, and wear is the inevitable result of friction. Although, in many cases, friction is a desirable or even essential physical phenomenon for moving objects (for example, during walking or when braking a vehicle), it is also the main cause of energy dissipation, material loss and equipment failure [1–3]. Friction also increases energy consumption and carbon emissions, which has severely hindered sustainable development progress [4, 5]. A drastic friction reduction in all branches of industry as well as in the transportation sector is expected to result in enormous energy savings and a sizable reduction in CO_2 emissions, but a fundamental understanding of friction is still a scientific challenge for the sustainable future of mankind [6, 7]. Currently, the concept of superlubricity has become a promising way to address the abovementioned issues, and developing effective lubricants is crucial for energy conservation and environmental protection because they can help establish a thin film to separate the sliding surfaces and lower the friction force.

Since the superlubricity concept was proposed in 1990, ultralow friction and near-zero wear are supposed to be the most ideal operating states of mechanical equipment. Compared with solid superlubricity, liquid superlubricity is less dependent on environmental conditions, such as atmosphere, temperature, and humidity, which pave the alternative ways for its sustainable development [8, 9]. Liquid superlubricity contains micro- and macro-scales based on the test instrument or the applied load level. At the microscale, superlubricity is primarily obtained on an atomically smooth surface, e.g., mica or graphene, by using surface force balance (SFB) or atomic force microscopy (AFM). The involved liquids are expected to be used in bio-lubrication, containing water, polymer brushes and liposomes [10]. The corresponding contact pressure is typically less than 10 MPa or up to 20 MPa in rare cases. At the macroscale, superlubricity is realized mainly in ceramics, glass, and steels, because these materials have high reactivity with hydroxy-containing groups, e.g., water, alcohols, and acids. Moreover, the above materials are widely used in engineering and industry, offering a well-established technological foundation and significant potential for further application. At present, numerous liquid-superlubricity systems have been found, but there are still major challenges considering the development of liquid superlubricity beyond the laboratory. The main challenges are concluded as insufficient level of friction reduction, low load-carrying capacity, velocity constraint, and long running-in period. Scientists have been working to develop effective compounds that exhibit superlubricity or even extremely low coefficients of friction (COFs) less than the ~10^{-3} level. A severe limitation of most superlubricity systems is that ultralow friction can be observed

[1] State Key Laboratory of Tribology in Advanced Equipment, Tsinghua University, Beijing 100084, China. [2] The Open University of China, Beijing 100039, China.

✉ Corresponding author. E-mail: chenxc1213@mail.tsinghua.edu.cn

Received: October 13, 2024; Revised: January 10, 2025; Accepted: February 4, 2025

only at a very small scale but can hardly be realized at the scale of macroscopic objects. For existing liquid superlubricity systems, it is generally accepted that their final contact pressure is less than 300 MPa. This view applies only to water-based lubricants rather than alcohols, oil-based lubricants, and diketones (DKTs). The excellent load-bearing capacity of water-based lubricants arises from the hydration lubrication mechanism, but it cannot be directly applied to oil-based lubricants. The high viscosity is beneficial for improving the load-bearing capacity of oil-based liquids but is contrary to achieving a low COF because of the high internal friction under hydrodynamic lubrication. Fortunately, high viscosity could promote boundary lubrication effects, which enable superlubricity at extremely low velocities or on a rough surface [11], offering great promise for the engineering development of oil-based superlubricity. In addition to the partial oil-based lubricants and hydrated ions that show superlubricity at a low velocity (e.g., ~0.8 mm/s for silicone oil [12]), most liquids will experience superlubricity failure at low velocity, which is a fatal flaw for devices that operate at low speeds or repeated start-stop conditions. The running-in process is another unexpected issue before achieving superlubricity. Different approaches have been developed to shorten the running-in period, but they are highly selective and only target specific superlubricity systems. In addition to the major shortcomings mentioned above, the influence of environmental conditions, particularly humidity, is still elusive, even though the frictional surfaces are completely immersed in the liquid. This phenomenon has been widely observed in water-based and oil-based lubrication. However, it is difficult to elucidate the mechanism for such limitations.

Therefore, the present work highlights the most recent developments in liquid superlubricity, with emphasis on the great challenges concerning the extension beyond the laboratory. In contrast to previous reports, detailed statistics have revealed the main limitations, i.e., insufficient level of friction reduction, low load-carrying capacity, velocity constraint, long running-in period, and severe wear loss, from the view of different types of lubricants and materials of friction pairs. The promising mechanisms to break through the above limitations are addressed. Specifically, a brief introduction to the development and exploration of liquid superlubricity is described in Section 2. The challenges in liquid superlubricity are discussed in Section 3, which are divided into four separate subsections concerning the main limitations. Eventually, the potential concepts and novel directions that enable to overcome current limitations are proposed in Section 4.

2 Discovery and exploration of liquid superlubricity

Figure 1 shows the discovery and exploration of liquid superlubricity. The generalized concept of liquid superlubricity should be dated back to 1938, when liquid superlubricity was referred to the superfluidity experienced with Helium-II as a liquid material at 2.172 K [13]. In 1987, Tomizawa and Fisher [14] found the extremely low COF (≤ 0.002) of water on Si_3N_4 self-mated pairs, which was the first study to show the "superlubricity" of water. Notably, the real concept of superlubricity was first defined in 1990 by Hirano and Shinjo [15] to describe a theoretical sliding regime in which friction and resistance completely vanished.

The developments of liquid superlubricity experienced water-based (denoted as water-b in Fig. 1) lubrication of ceramics (1987) [14], polymer brushes (2001) [16], oil-based (denoted as oil-b) lubrication (2005) [17], alcohols lubrication (2008) [18], liposomes (2008) [19], acid-based (denoted as acid-b) solutions or their mixtures with alcohols (2011) [20], and ionic liquids (ILs) lubrication (2014) [21]. Since the first discovery of superlubricity

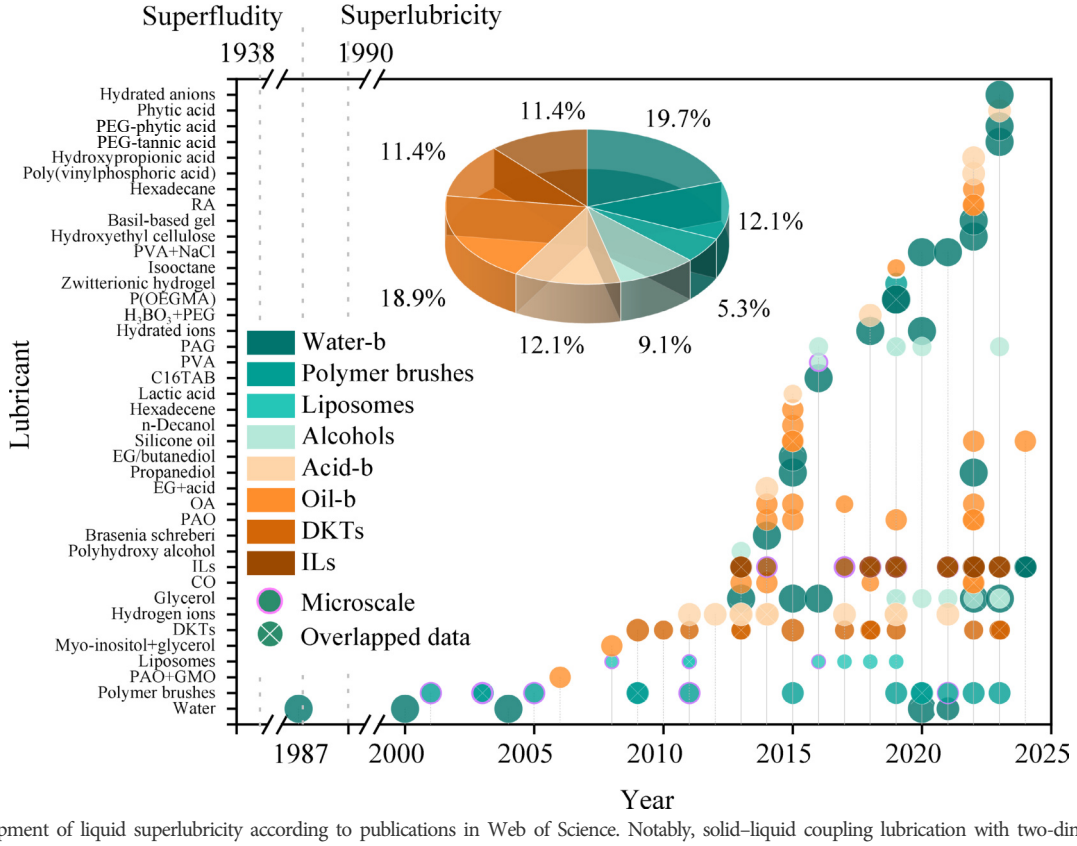

Fig. 1 Development of liquid superlubricity according to publications in Web of Science. Notably, solid–liquid coupling lubrication with two-dimensional (2D) materials is beyond focus of present work; *Y* axis roughly ranges over time; diameter of data point represents proportion of current lubricant used in the research.

of water on Si_3N_4 pairs, other ceramic tribopairs (SiC, CN_x, Al_2O_3, SiC with amorphous carbon (a-C), a-CN_x, and BCN coatings) [22–24] and factors (surface roughness [25], micro-pits [26], surface texture [27]) have been considered in the subsequent research on water superlubricity. In the following 20 years, as novel lubricants for bio-lubrication at the macroscale, polymer brushes received extra attention because of their extremely low COFs [28, 29]. The outstanding lubrication performance of polymer brushes was first reported by Klein's group [16]. Their results revealed an extremely low COF of 0.003 using SFB measurements. Liposomes are other effective lubricants that exhibit superlubricity, particularly under boundary conditions, and were initially found as early as 2008 [30]. Trunfio-Sfarghiu et al. [19] found that dipalmitoylphosphatidylcholine (DPPC) bilayer showed a super-low COF of 0.002 between glass and hydroxyethyl methacrylate (HEMA) surfaces using a home-made tribometer. The fundamental research on water-based ceramic lubrication, polymer brushes, and liposomes is relatively mature, accounting for approximately 37% of liquid superlubricity. Note that the acid-based lubricants accounting for 12.1% should also be considered into the ratio calculation of water-based lubricants. These lubricants are difficult to use directly in engineering lubrication because of their corrosion, instability, and lower load-bearing capacity. Therefore, non-aqueous liquid lubrication has received widespread attention at the same time. The oil-based liquid is the medium that is most closely linked with industrial and engineering lubrication, but its superlubricity is strictly restricted in specific situations or conditions. The first superlubricity of oil-based liquids was achieved on substrates with special coatings. In 2005 and 2006, Kano [17] studied the superlubricity of glyceryl monooleate (GMO) and poly-alpha-olefin (PAO) between steel pins and tetrahedral amorphous carbon (ta-C)-coated films. An ultralow COF of 0.006 at a sliding speed of 0.1 m/s was obtained. In 2008, Matta et al. [18] further revealed the superlubricity and tribochemical reactions of polyhydric alcohols at steel surfaces and/or ta-C-coated surfaces. It is the first time to achieve ultralow friction (< 0.01) of steel under boundary lubrication in the absence of long-chain polar molecules.

The research on superlubricity was initially at the microscale and was conducted on atomically smooth surfaces using a surface force apparatus (SFA) and AFM before 2010, after which breakthroughs were made in macroscale superlubricity. Pioneering progress has been achieved through acid-based liquids, such as acidic aqueous solutions (H_3PO_4 [20, 31], H_3BO_3 [32], lactic acid [33, 34], etc.), mixtures of inorganic acids and polyhydroxy alcohol between glass and Si_3N_4, sapphire and sapphire, and Si_3N_4 and sapphire tribopairs under a normal pressure lower than 300 MPa [35]. Thereafter, Zhang et al. [36] explored the superlubricity of mixtures of boric acid and glycerol on glass plates and Si_3N_4 balls after a running-in process of a few minutes. Li et al. [37] explored the superlubricity of glycerol by mixing it with different acid solutions, such as hydrochloric acid (HCl), lactic acid ($C_3H_6O_3$), oxalic acid ($H_2C_2O_4$), citric acid ($C_6H_8O_7$), and sulfamic acid (H_3NO_3S). It was found that all these acids could achieve superlubricity when mixed in a glycerol solution. Additionally, they further explored the superlubricity of acids and alcohols with different numbers of hydroxyl groups. The results first demonstrated that the number of hydroxyl groups no less than 2 is essential for achieving superlubricity, but the number of carbon atoms and the arrangement of hydroxyl groups seem to have no obvious effect. Since then, the superlubricity mechanism of alcohols mixed with acidic solutions has been fully elucidated. The fluid-hydrated water layer between the hydrogen-bonded networks of alcohols and water molecules on the positively charged surfaces was responsible for the beneficial effects of the above systems. The discovery of ultralow friction (< 0.005) in DKTs was originally derived from studies on the lubrication properties of liquid crystalline fluids, which have been discussed for 30 years [38–40]. In 2009, Amann and Kailer [41–43] systemically studied the ultralow friction behavior of DKTs on 100Cr6 self-mated surfaces using an SRV (Schwingungs Reihungund Vderschleiss) tribometer and revealed the corresponding lubrication mechanism. Notably, DKTs, as liquid crystalline fluids, are generally denoted as mesogenic fluids (MFs) at the initial stage. In 2013, Walter et al. [40] first demonstrated the assumption that the ultralow friction of DKTs was connected to the formation of iron complexes using gradient-corrected density functional theory (DFT). Since then, the use of DKTs, accounting for 11.4%, as oil-based lubricants or additives has become a novel research hotspot. Moreover, as special lubricants consisting of anions and cations, ILs exhibit exotic lubrication performance both as neat lubricants and as additives in water, oils, or greases for metals and ceramic materials under severe conditions, but their COFs are often greater than 0.01 at the macroscale [21, 44–47]. In 2013, Espinosa et al. [48] revealed the superlubricity of a protic ionic liquid under the contact of sapphire/316L stainless steel (SS) with its minimum COF down to 0.0001 (the mean COF was 0.02). This discovery came a decade after ILs were first used as lubricants in 2001 by Ye et al. [49].

As overviewed above, liquid superlubricity has experienced development from micro- to macro-scale, from water to diversified types, e.g., water-based lubricants, alcohols, acid-based lubricants, oil-based lubricants, and ILs. Water-based and oil-based lubricants as well as ILs are more promising directions for achieving industrialization, which thus become the core focus at present. Importantly, how to realize the transformation from laboratory to engineering applications still faces considerable challenges.

3 Challenges in liquid superlubricity

Since the concept of superlubricity was first proposed, a large number of liquid compounds with superior lubricities have been discovered, and different mechanisms have been established. Under microscale conditions, biomaterials, such as water, polymer brushes, and liposomes, have been characterized via SFB and AFM. Under macroscale conditions, more materials with ultralow friction have been found, including water, alcohols, hydrated materials, acid-based solutions or their mixtures with alcohols, oil-based lubricants and ILs. Many researchers have focused on establishing mechanisms for achieving superlubricity in different systems. However, the development of liquid superlubricity is not mature enough, and there are still elusive problems to overcome. Insufficient friction reduction, low load capacity, velocity constraints, long running-in period, and severe wear loss are common concerns. The influence of environmental conditions on achieving superlubricity, particularly humidity, seems elusive even if the frictional pairs are completely immersed into liquid during frictional tests. Therefore, this section presents an overview of the challenges in liquid superlubricity based on the types of superlubricity liquids and the materials of friction pairs, with an emphasis on those at macroscales, including water-based lubricants, alcohols, acid-based lubricants, oil-based lubricants, DKTs, and ILs, as shown in Table 1. Notably, the current classification is not completely rigorous and should be handled with care. DKTs act as oil-based additives but are divided into a separate category as a novel focus in the latest research. In the process of data statistics, the referred materials of friction pairs are

Table 1 Typical liquid superlubricity systems and corresponding classification in present work

Type	Lubricant	Friction pair
Microscale	Water	Zwitterionic copolymer hydrogel and sapphire [50]
	Polymer brushes	Hydrophobized mica [51]; mica [52, 53]; half-silvered mica [54]; bottlebrush polymers [55]; PDMS [56]; GCr15/SiO_2 [57]; Si_3N_4 [58]
	Phytic acid	PDMS/SiO_2 [59]
	Liposomes	Borosilicate glass/hydroxy ethyl methacrylate [19]; HSPC–SUV coated mica [60]; mica [61, 62]; SiO_2 [63]; SiO_2/graphene [64]; polystyrene/Ti6Al4V [65]
	Hydroxyethyl cellulose	Quartz [66]
	Hexadecyltrimethylammonium bromide	SiO_2 [67]
Water-based	PVA and NaCl [68, 69]; hydrated ions [70–72]	Si_3N_4/sapphire
	$PAG_{(aq)}$	Si_3N_4/sapphire [73, 74]; Si_3N_4/Al_2O_3 [75]
	P(OEGMA) [76]; Basil-based gel [77, 78]	Si_3N_4/Al_2O_3
	$Glycerol_{(aq)}$	GCr15 [79]; sapphire [80]; Si_3N_4 [81]; Si_3N_4/TiO_2 [82]
	Ethanediol; butanediol; propanediol	Sapphire [80]
	Lithium $citrate_{(aq)}$+EG	Si_3N_4/a-C [83]
Alcohols	PAG	Si_3N_4/Al_2O_3 [84]; GCr15 [85]
	Glycerol (80 °C); myo-inositol+glycerol (25 °C)	DLC [18]
	Glycerol; propanediol	GCr15/DLC [86, 87]; Si_3N_4/graphene–SiO_2 [88]; Si_3N_4 [89]; GCr15 [90]
Acid-based	H^+ [33, 34];	Si_3N_4/SiO_2
	PVPA	Ti6Al4V/PTFE [91]
	Hydroxypropionic acid	GCr15/DLC [92]
	HCl	Si_3N_4/PCD [93]
	H_3PO_4	Si_3N_4/glass [20, 94]; Si_3N_4/sapphire [95]; Si_3N_4/SiO_2 [96–100]; sapphire [20, 101]
	Acid (H_3BO_3 [32], tannic acid [102], phytic acid [59], etc.)+$alcohols_{(aq)}$ [35, 103]	Si_3N_4/SiO_2
Oil-based	Silicone oil	Sapphire [80]; Si_3N_4/sapphire [104]; Si_3N_4/SiO_2 [12]
	RA	GCr15/Si_3N_4 [105]
	PAO+GMO	GCr15/DLC [17]
	PAO	Al_2O_3/TiB_2–MoS_2 [106]; GCr15 [107]
	OA	DLC [108]; GCr15/DLC [109]; sapphire [80]
	n-Decanol	Sapphire [80]
	CO	DLC/Si_3N_4 [110]; GCr15/DLC [111]; Nitinol 60/GCr15 [112, 113]
Diketones	1,3-Diketones	GCr15 [11, 40–43, 114–120]; SS [121]
	Ethylacetophenone solutions with benzoyl acetone	GCr15 [122]
ILs	FA-IL, PA-IL, IA-IL, TA-IL	GCr15 [123]
	N,N-Dimethyldodecylamine and N-octanoic acid or decanoic acid	PTFE/SS [124]
	Bis(2-hydroxyethylammonium) succinate or its aqueous solution	Sapphire/SS [48]
	1-Butyl-2,3-methylimidazolium tetrafluoroborate in PEG_{aq}	Si_3N_4/sapphire [125]
	[Li(EG)]$PF_{6\ (aq)}$, [Li(EG)]$BF_{4\ (aq)}$, [Li(EG)]$NTF_{2\ (aq)}$, and [Na(EG)]-$PF_{6\ (aq)}$	Si_3N_4 [126]
	$[EMIM]TFS_{(aq)}$	Si_3N_4/SiO_2 [127]
	Ionic liquid polymer brush	SiO_2/Si [128]

* Self-mated friction pairs only show one material; full names of partial lubricants or friction pairs are given in the text. a-C: amorphous carbon; P(OEGMA): poly(oligo(ethylene glycol) methylether acrylate); PDMS: polydimethylsiloxane; HSPC–SUV: hydrogenated soy phosphatidylcholine–small unilamellar vesicle; PVA: poly(vinyl alcohol); PAG: polyalkylene glycol; DLC: diamond-like carbon; PVPA: poly(vinylphosphoric acid); PTFE: polytetrafluoroethylene; PCD: polycrystalline diamond; RA: ricinoleic acid; PAO: poly-alpha-olefin; GMO: glyceryl monooleate; OA: oleic acid; SS: stainless steel; [EMIM]TFS: 1-ethyl-3-methylimidazolium trifluoromethanesulfonate; FA: 2,5-furandicarboxylic acid; PA: phthalic acid; IA: isophthalic acid; TA: terephthalic acid; EG: ethylene glycol.

unified, where 100Cr6 steel and AISI52100 steel are denoted as GCr15 for their approximate mechanical properties (the replacement has been performed in Table 1); sapphire is denoted as Al_2O_3; silica glass and quartz are considered SiO_2.

3.1 Insufficient level of friction reduction

Researchers have found a large number of liquid compounds with superlubricity properties, but these liquids are limited to only water, polyols, inorganic acids, unsaturated fatty acids, olefins,

DKTs, and ILs, so how to extend the superlubricity to more substances is still a huge dilemma. These liquids exhibit high selectivity to friction pair materials. Water-based superlubricity is more prevalent in ceramic materials, while oil-based liquids mainly have ultralow friction on surfaces containing specific coatings (e.g., DLC) and on GCr15 self-mated surfaces, which typically has a long running-in period before superlubricity is achieved. Additionally, concerning macro-superlubricity, the COF is usually higher than ~0.004, and how to achieve a lower COF or even at the ~10^{-4} level seems out of reach. Figure 2 shows the COF distributions of the liquid superlubricity systems classified by different types of liquids and different materials of friction pairs. At the microscale, superlubricity is mainly established on mica surfaces with atomically smooth surfaces, and their COFs are as low as 0.0004 (e.g., lubricated by polymer brushes) [52, 53]. When mica surfaces are coated with small unilamellar vesicles (SUVs) of hydrogenated soy phosphatidylcholine (HSPC) lipids and then slid under water lubrication, the COF can be as low as 0.00002. Such ultralow COFs could even be comparable with solid superlubricity [60]. Hexadecyltrimethylammonium bromide (C16TAB) exhibited an ultralow COF of 0.0007 between SiO_2 self-mated surfaces at a normal load of 3.6 MPa [67]. The traditional engineering materials of GCr15 can also show an ultralow COF of 0.0006 under the lubrication of polymer brushes when it is mated with SiO_2 [57]. However, such extremely low friction can hardly be realized at the macroscale. At the macroscale, an ultralow COF is typically obtained on ceramics, particularly on Si_3N_4 and sapphire surfaces, when lubricated with aqueous solutions. Water-based lubricants and alcohols exhibit excellent superlubricity, and their COFs typically range between 0.002 and 0.006. The lowest COF occurred due to the lubrication of hydrated ions on Si_3N_4 and sapphire, particularly trivalent ions, such as $AlCl_3$, $CeCl_3$, and $CrCl_3$ [71, 129]. It has been demonstrated that the hydration repulsion force not only improves the load-bearing capacity of liquid superlubricity but also results in an easier-shearing layer with the formation of a very hard hydration shell by the cations, thus effectively decreasing the COF. Poly(vinyl alcohol) (PVA) aqueous solution containing NaCl shows ultralow COFs of 0.0017 or 0.0023 on the surfaces of Si_3N_4 and sapphire. The contact pressure can reach 717 MPa [68, 69]. The hydrated Na^+ ions play a significant role in enhancing the hydration repulsion force and providing low shear stress between the solid surfaces. The hydration effect can also enhance the lubrication effect of polymers without saline ions. The free water molecules effectively weaken the interactions between polymer chains, and the hydrogen-bonded polyalkylene glycol (PAG) chains form a hydrated layer between two sliding solid surfaces to lower the shear strength. The PAG aqueous solution has ultralow friction on Si_3N_4 and sapphire surfaces, and the COF can be as low as 0.0023. For acid-based solutions, the research on the superlubricity performance of H_3PO_4 aqueous solution is the most mature, and an ultralow COF of 0.003 can be achieved on Si_3N_4 and sapphire or SiO_2 [20, 95, 97, 100].

Oil-based lubricants commonly show a higher COF than water-based lubricants and alcohols. High viscosity might be one of the most important reasons for such high COF distributions. The lowest COF of 0.003 was observed on the GCr15 and Si_3N_4 surfaces when lubricated with ricinoleic acid (RA) [105]. The same COF also occurred on the Si_3N_4 and Si_3N_4 surfaces because of the lubrication of n-decanol, but it occurred under a lower final contact pressure of 49 MPa than the above lubrication of RA at 146 MPa. DKTs, as oil-based lubricants, show high COFs between 0.004 and 0.008, and their long running-in periods are the main concern. Pure ILs exhibit superlubricity on the surfaces of GCr15 and GCr15 [127], PTFE and SS [124], DLC and DLC [130], etc. The high viscosity of pure ILs limits the hydrodynamic effect in the friction process. Thus, their aqueous solutions are more accessible to achieve superlubricity on multiple friction pairs, such as GCr15 and GCr15 [123, 131], Si_3N_4 and Si_3N_4 [126], Si_3N_4 and sapphire [125], Si_3N_4 and SiO_2 [127], sapphire and SS [48], etc. The lower COF occurred for the ILs' aqueous solution on the Si_3N_4 and SiO_2 surfaces, with the COF reduction down to 0.002 [127], and that on Si_3N_4 self-mated surfaces was 0.003 [126], and that on GCr15 self-mated surfaces was 0.0035 [123]. This ultralow friction not only depends on the excellent lubrication effect of ILs but also has to do with the viscosity decrease and hydration force by water.

3.2 Limitation of low load-carrying capacity

The load-carrying capacity of liquid superlubricity systems has been greatly improved over the past few years. Figure 3 shows the distributions of contact pressure and contact pressure reduction for different liquid lubricants and friction pairs. The typical contact pressure closely depends on the type of liquid and the materials of friction pairs. The difference between the initial contact pressure (ICP, i.e., the maximum contact pressure, or initial Hertz contact pressure) and final contact pressure (FCP, i.e., the contact area divided by the normal load) results from severe wear in the running-in process, and a higher value of FCP/ICP indicates a lower reduction in contact pressure. It is generally

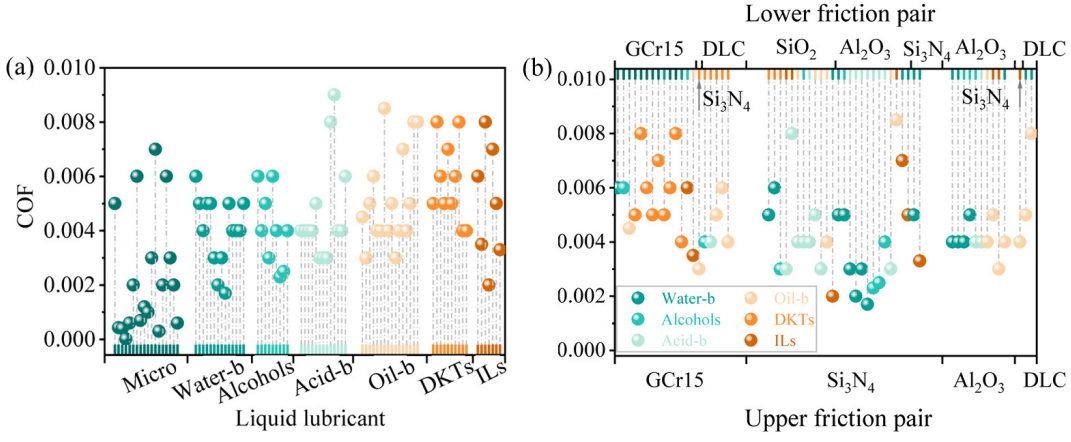

Fig. 2 COFs for different liquid superlubricity systems: classified by (a) lubricants and (b) friction pairs. Notably, sapphire and glass are denoted as Al_2O_3 and SiO_2, respectively, because of their similar compositions. Upper and lower friction pairs correspond to ball/pin-on-disk configurations in most common friction tests. Same methods are adopted in following sections.

suggested that the FCP is less than 300 MPa, even if the ICP is as high as 1 GPa; however, in fact, the FCP of oil-based lubricants is not higher than 200 MPa [119], and that of diketone is only approximately 100 MPa even with the help of its chelate [119], as shown in Fig. 3(a). The striking reduction in contact pressure is an unexpected issue and is caused by violent wear at the beginning of the running-in period. Taking the FCP/ICP as a measure, as shown in Fig. 3(b), water-based lubricants show the highest level of FCP/ICP, which is slightly greater than 30%, and extremely low levels occur in most types of superlubricity liquids containing oil-based lubricants (FCP/ICP ratio of approximately 10%). From the perspective of materials of friction pairs, as shown in Figs. 3(c) and 3(d), the Si_3N_4 and Al_2O_3 (sapphire) pairs show high final contact pressures, especially when lubricated with water-based lubricants, and the FCP/ICP can reach ~35% or even ~85%. When Si_3N_4 is mated with itself or SiO_2, both the ICP and the FCP decrease. The self-mated GCr15 pairs or those with DLC surfaces are commonly used in the lubrication of DKTs and oil-based lubricants; thus, the contact pressure is predictably low. Solid–liquid coupling with 2D materials, such as graphene [132], boron nitride [133], and black phosphorus [134, 135], is the prevailing way to improve the load-carrying capacity of materials, and the superlubricity could be feasibly realized at final contact pressures of up to 600 MPa [69, 136]. Liquid superlubricity is affected by both the contact pressure and the pressure–viscosity coefficient of the lubricant. However, on the basis of the Hammock–Dowson theory, the load-carrying capacity of a liquid may reach 500 MPa when the pressure–viscosity coefficient of the liquid lubricant is below the GPa^{-1} level. Notably, liquid superlubricity without any solid additives still has many potential for relieving the limitation of the load-bearing capacity. This section discusses the mechanism and methods used to improve the load-bearing capacity independent of 2D materials.

In the field of microscale research, mica or graphene sheets with atomically smooth surfaces and biological materials are adopted as friction materials. Water, polymer brushes, and liposomes have become the main focus, and they are expected to be used in biological lubrication. Microscale superlubricity is typically carried out using nano-tribological devices, e.g., SFB, and AFM, and the involved FCP is typically limited to 7.5 MPa [53, 56]. As is well-known, natural joints are in a well-lubricated environment, with a COF of 0.001–0.01 and an average bearing capacity of ~5 or ~20 MPa in some situations [30, 65, 137]. The excellent performance of polymer brushes and liposomes is attributed primarily to the adaptability of elastic articular cartilage and the brush-like structure of water-soluble macromolecules in synovial fluids [137]. Goldberg et al. [60, 61] prepared SUVs of HSPC liposomes. Liposomes were self-assembled in close-packed layers on mica surfaces and achieved an extremely low COF of 0.00002–0.0001 under water conditions and a contact pressure of more than 12 MPa. Vlădescu et al. [57] exploited the synergy between concentrated polymer brushes (CPBs) and laser surface texturing to achieve durable superlubricity using a custom-built tribological apparatus. The combination of CPBs with a laser-produced surface texture reduced the COF to 0.0006 at a low speed of 0.2 mm/s and increased the durability of CPBs by up to 34%. The textured micro-features could offer lateral support, and the corresponding contact pressure reached 25 MPa. Polymer brushes also show ultralow lubrication performance at the macroscale. Müller et al. [138] explored the effects of molecular architecture on the macroscopic lubrication properties of the brush-like co-polyelectrolyte poly(L-lysine)-g-poly(ethylene glycol) (PLL-g-PEG) between SS/glass surfaces. A feasible superlubricity was achieved at a maximum Hertzian contact pressure of 410 MPa. Notably, the experiment was carried out in a mixed sliding/rolling

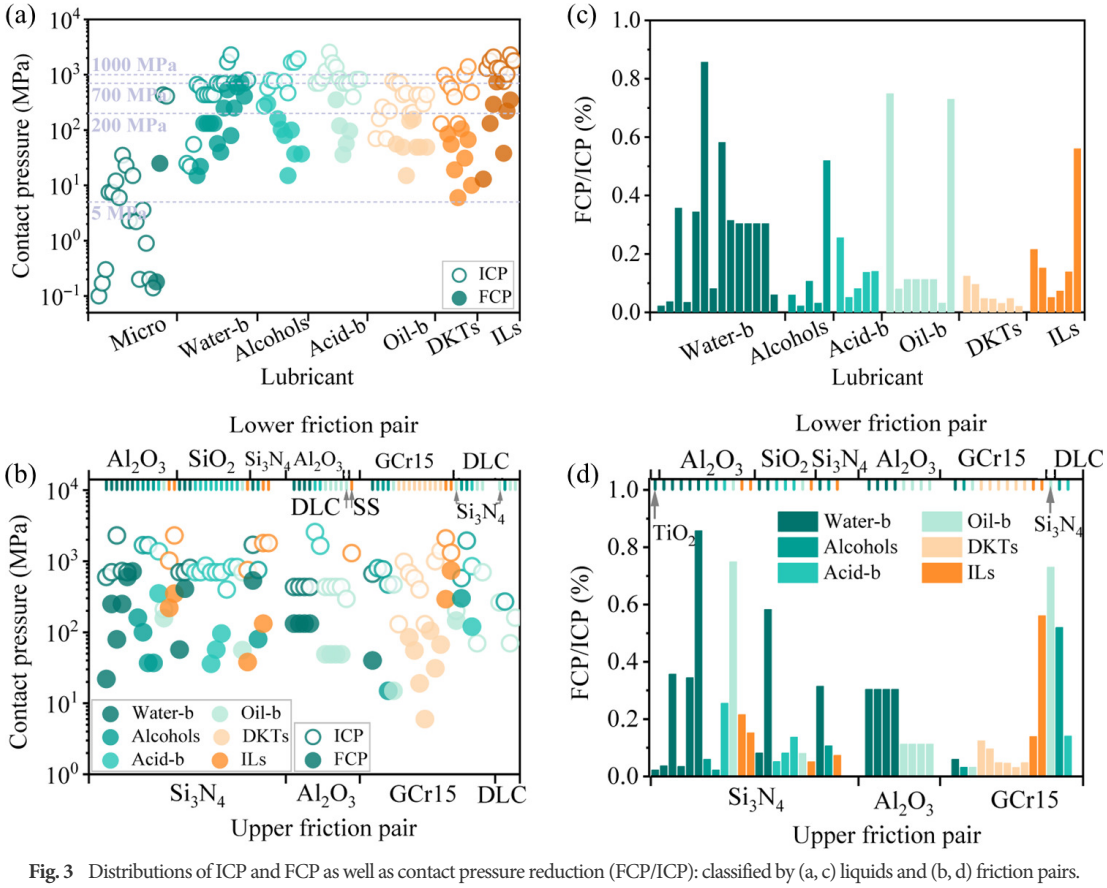

Fig. 3 Distributions of ICP and FCP as well as contact pressure reduction (FCP/ICP): classified by (a, c) liquids and (b, d) friction pairs.

contact regime using a mini-traction machine. The combination of ILs with polymer brushes has been justified as a successful method to increase the load-carrying performance of polymer brushes. Arafune et al. [128] achieved superlubricity on a smooth glass ball (SGB)/ionic liquid polymer brush (ILPB), and the prepared ILPB was grafted onto a Si surface. This ultralow friction could be maintained under an average contact pressure of 434 MPa. Compared with a previous report on an ILPB/ILPB with a relatively high COF under mixed lubrication, the author noted that the improvement in surface roughness in the SGB/ILPB system was conducive to extending the range of hydrodynamic lubrication, inhibiting abrasive wear and then contributing to the expression of superlubricity.

For the macroscale superlubricity of liquid lubricants, the applied friction pairs are usually glass, ceramic, and steel, which are most widely used in industry [139, 140]. These materials usually have high hardness or high reactivity with specific liquid lubricants. At present, the FCP is generally less than 300 MPa, but in fact, this only applies to earlier studies of water-based solutions. For the aqueous solutions as shown in Fig. 3(a), such as water-based liquids, mixed alcohols in acidic solutions, and alcohol-based liquids, the ICP is as high as 1 GPa, and the FCP is commonly more than 700 MPa [69], even up to 1 GPa in rare cases [83]. Water or neat alcohols generally have low load-bearing performance, and hydrated ions are effective species for improving the load-bearing performance of aqueous lubricants. Han et al. [141] realized superlubricity with an ultralow wear rate after a rapid running-in period (< 1 min) by mixing hydrated ions into a PEG solution. A high FCP/ICP ratio of approximately 0.8 was observed, where the ICP was 700 MPa and the FCP was above 550 MPa. Li et al. [69] propelled a novel route for achieving extreme-pressure superlubricity by enhancing the superlubricity of polymer solution with hydrated salt ions. In their report, an aqueous solution consisting of PVA and NaCl exhibited excellent superlubricity (μ = 0.0017) between Si_3N_4 and sapphire under extreme pressure (717 MPa), but the polymer solution alone had no superlubricity. The author suggested that the superlubricity of the PVA/NaCl mixture is attributed to the combination of hydration and hydrodynamic effects. NaCl enhanced the hydrodynamic effect by increasing the viscosity of the polymer solution. The competitive adsorption between hydrated Na^+ ions and PVA molecules resulted in the transformation of the shear interface from a polymer film/polymer film to a solid/polymer film. The beneficial effect of hydrated ions in improving the load-bearing capacity has been confirmed by molecular dynamic simulations. The high load-bearing capacity of hydrated ions resulted from a repulsive hydration force and the cations formed a very hard hydration shell. Sun et al. [83] achieved superlubricity between Si_3N_4/a-C mating parts by the lubrication of lithium citrate (LC) and EG aqueous solution. This is the first study to show superlubricity under extremely high contact pressure (ICP = FCP = 1.15 GPa), and the reduction in contact pressure is almost negligible due to near-zero wear. It was inferred that mechanical shearing promoted chemisorption of the LC molecules between the carboxylate radicals and the a-C film. The exposed lithium ions caused the formation of a hydration layer, providing extremely low shear strength, and the colloidal silica layer could also reduce friction. Jia et al. [76, 142] synthesized a novel comb-typed poly(oligo(ethylene glycol) methylether acrylate) (P(OEGMA)) via reversible addition–fragmentation chain transfer (RAFT) polymerization and studied its tribological properties in aqueous solutions on Si_3N_4 and Al_2O_3 surfaces. Compared with commercial linear PEG, the uniformly smaller size of P(OEGMA) led to a decrease in viscosity in aqueous solutions. An ultralow COF was realized at an ICP of up to 2,300 MPa, and the FCP was higher than 300 MPa. The excellent lubricating performance is attributed to the good adsorption property of P(OEGMA), and the high load-carrying capacity is attributed to both the hydration force and hydrodynamic effects. However, the evident decrease in contact pressure with an FCP/ICP value lower than 13% is essential to achieve superlubricity, but that is not what researchers expect. The improvement of the load-carrying capacity using the hydration force is feasible for aqueous liquids, but this does not apply to non-aqueous solutions, such as oil-based lubrication, DKTs, and pure ILs.

For the superlubricity of oil-based liquids, tribological reactions and hydrodynamic effects play a predominant role in bearing the normal load. Their ICPs are generally no more than 700 MPa. Kano [17] studied the ultralow friction of a ta-C film applied to an engine cam follower lubricated with PAO oil containing 1 wt% GMO under contact with three-pin on disk surfaces under boundary lubrication. A high ICP of 700 MPa was applied to accommodate the actual contact pressure of cam follower, and this was the first time that DLC lubricated with an ester-containing oil showed superlubricity. Li et al. [12] realized the superlubricity of silicone oil between Si_3N_4/SiO_2 surfaces after running-in with an acid solution. The ICP can reach 700 MPa, but the FCP significantly decreases to 56 MPa. The resulting value of FCP/ICP is as low as 0.08. In the running-in process, the hydrogen ions caused the formation of a circular plane. An evident reduction in both the contact pressure and COF occurred in the mixed lubrication regime, facilitating the superlubricity of silicone oil in a hydrodynamic state. Wen et al. [104] realized high-temperature superlubricity with chlorinated-phenyl and methyl-terminated silicone oil (CPSO) after hydrogen-ion running-in under high load conditions. For the first time, superlubricity of oil-based superlubricity was achieved at temperatures of 190 °C, or even higher temperatures, and the maximum contact pressure was approximately 200 MPa. The running-in process with H^+ ions improved the adsorption capacity of CPSO on the hydroxylated SiO_2 surface and decreased the steric hindrance, while high temperature caused a critical reduction in both the viscosity and pressure–viscosity coefficient of CPSO, thus facilitating the achievement of superlubricity predominated by the hydrodynamic effect. Ge et al. [85] reported the superlubricity of both polar molecules PAG and nonpolar molecules PAO on the contact of GCr15/GCr15 surfaces pretreated with PEG aqueous solution. A tribochemical layer composed of oxides, iron oxides, FeOOH, and $Fe(OH)_3$ was formed by PEG_{aq} treatment, during which severe wear caused the contact pressure to drop from 700 to 15 MPa; however, once superlubricity was established, no wear occurred. The pre-treatment facilitates the realization of superlubricity, but the extremely low real contact pressure limits its extension beyond the laboratory. Li et al. [80] compared the effects of water- and oil-based superlubricity on self-mated sapphires. Their experiments revealed that the superlubricity of water-based lubricants, including glycerol solution (70%, v/v), ethanediol solution (100%, v/v), 1,3-propanediol solution (90%, v/v), and 1,4-butanediol solution (90%, v/v), can be achieved even when the average contact pressure was higher than 100 MPa, while that of oil-based lubricants, including OA, PAO 4, silicone oil and n-decanol, can be obtained only when the pressure was reduced to 50 MPa. It was suggested that this difference in superlubricity was essentially linked to the pressure–viscosity coefficient of two types of lubricants. The pressure–viscosity coefficient must be as small as possible to obtain superlubricity at higher pressures, while that can be achieved with a broad range of pressure–viscosity coefficients at lower pressures. Therefore, for oil-based lubricants in mixed or

hydrodynamic lubrication states, a low viscosity and a pressure–viscosity coefficient are expected. However, when it is involved in boundary lubrication, high viscosity is beneficial for avoiding the direct contact of asperities and improving the load-carrying capacity.

As an oil-based lubricant or additive, the superlubricity of DKTs is primarily obtained between the surfaces of GCr15 and GCr15[120]orevenDLCfilms[143,144].TheICPcanreach1,400MPa, but the FCP rarely reaches 100 MPa [11, 121]. Yuan et al. [120] studied the critical load of 1,3-diketone oil (1-(4-ethyl phenyl) nonane-1,3-dione, EPND) to achieve superlubricity on steel surfaces. The results revealed that the superlubricity of 1,3-diketone can be obtained at a load threshold of 600 MPa < $P \leqslant$ 1,400 MPa at a velocity of 300 mm/s, but the FCP is as low as 67 MPa. A lower load caused insufficient running-in, which could not ensure good asperity level conformity of frictional pairs, but a higher load produced excessive wear and debris. In the research of Liu et al. [116], an ultralow friction (μ = 0.008) of 1,3-diketone was obtained at the same surfaces under a normal load of 980 MPa. Although the ICP achieving superlubricity can reach a heavy load level, the FCP was still far away from 200 MPa. Li et al. [115] realized the superlubricity of 1,3-diketone on steel surfaces with a roughness of engineering level. On the surfaces with arithmetic mean height Sa = 17 nm and Sa = 202 nm, the contact pressure that achieves superlubricity decreases from an initial value of 1,000 to 31 and 21 MPa, respectively. Li et al. [117] and Du et al. [119] demonstrated that the FCP of 1,3-diketone could reach high values of 84.8 and 105.2 MPa, with an approximate COF of approximately 0.006. In addition, the chelate of ferric chloride and 1,3-diketone results in a high contact pressure of 161.4 MPa when it combines with the PAO base oil in the lubrication of steel friction pairs [145, 146]. However, the weak protection of DKTs corresponding to a significant decrease in contact pressure is still a major challenge.

Both ILs and their aqueous solutions are effective lubricants for achieving ultralow friction. The superlubricity of ILs is typically obtained at an ICP of up to 1 GPa. Chen et al. [123] revealed the macroscale superlubricity of GCr15/GCr15 contact by polymer-based ionic liquids (PILs) that were synthesized with the same polymeric amine cation (Jeffamine M2070) and different anions, including 2,5-furandicarboxylic acid (FA), phthalic acid (PA), isophthalic acid (IA), and terephthalic acid (TA). All ILs showed excellent superlubricity without a running-in period, and the ICP reached 1.32 GPa. The experiment was carried out on a four-ball tribometer that acts as an industrial instrument for lubricating performance evaluation. The authors attributed these beneficial effects to the flexible and electron-rich polymeric chain of the synthesized PILs and the formation of a robust tribofilm. Zheng et al. [131] reported the superlubricity of protic ionic liquids in propylene glycol aqueous solution over wide load and velocity ranges on GCr15 surfaces. The ICP reached 2.1 GPa, and the FCP was 292 MPa. The results confirmed that the hydrogen bond network between the polyol aqueous solution and hydrogen ions was the main reason for the excellent load-bearing capacity. ILs with longer alkyl chains participated in the tribochemical reaction with the GCr15 surfaces, and water caused the friction reduction of polyols and enabled superlubricity to be realized at high-speed rotations.

3.3 Velocity constraint

Another important concern in liquid superlubricity is the velocity constraint, which has limitations at both low and high velocities. The velocity constraint can be explained to some extent by the classical Stribeck theory. At a low speed, lubrication is in the boundary lubrication state, which is dominated by the interface characteristics, such as roughness and mechanical properties. The inevitable differences in asperity level conformity between two frictional surfaces commonly cause severe surface damage and high COFs [139]. At high speeds, the strong mechanical shear possibly stimulates the decomposition of lubricant molecules (mechanochemical reactions) or changes in physiochemical performance. Moreover, high speed also means an insufficient running-in process [147]. All these factors could lead to superlubricity failure. The viscosity of superlubricating lubricants is typically lower than 45 mPa·s (accounting for approximately 72%) or even lower than 15 mPa·s (accounting for approximately 49%) because of the dominant role of hydrodynamic lubrication in achieving superlubricity, as shown in Figs. 4(a) and 4(b). The aqueous solution typically has a low viscosity but cannot withstand high contact pressure, so a hydrodynamic effect is needed to separate the friction surfaces, and an ultra-low COF is achieved because of the low shear internal stress (Fig. 4(c)). This regime has been applied to achieve superlubricity of ILs. For some pure ILs with high viscosities, it is difficult to achieve superlubricity on their own, but their aqueous solutions with suitable concentrations exhibit ultralow COFs. Notably, although the aqueous solutions cannot provide enough load-bearing capacity because of their relatively low viscosity, the hydration effect provides additional support when compared to non-aqueous solutions. Oil-based lubricants with high viscosity (e.g., silicone oil, 100–1,000 mPa) or glycerol (~934 mPa·s at room temperature) have relatively high load-carrying capacity and are not sensitive to changes in load or surface roughness (R_a) (Fig. 4(d)). Their superlubricity is predominantly achieved in the boundary or mixed lubrication state, and an increase in viscosity (e.g., by lowering the temperature) is conducive to improving the ability of the friction surface separated, while in the hydrodynamic lubrication state, lubricants with a high shear internal stress lead to superlubricity failure. As a non-Newtonian fluid, the viscosity of DKTs experiences shear thinning and autonomously accommodates over a wide range of velocities, which is conducive to achieving superlubricity under hydrodynamic lubrication.

Figure 5 shows the distribution of velocity to achieve superlubricity for different lubricants or friction pairs. Note that the mentioned typical velocity refers to a specific speed to achieve optimal superlubricity performance, e.g., the minimum COF and maximum final contact pressure. The velocity to achieve superlubricity is significantly affected by the type of lubricant. The typical ranges for water-based lubricants, pure alcohols and acid-based lubricants are between 20 and 250 mm/s, but a higher velocity range from 100 to 560 mm/s occurs for DKTs, and a velocity range from 50 to 250 mm/s occurs for ILs. From the perspective of different materials of typical friction pairs, self-mated GCr15 pairs show a high level of velocity distribution between 100 and 500 mm/s, because such friction pairs are commonly adopted for the superlubricity of DKTs. Si_3N_4 and sapphire are effective surfaces for the superlubricity of water-based lubricants and pure alcohols, which are accompanied by a relatively low level of velocity distributions, namely, 20–100 mm/s. The self-mated Si_3N_4 surfaces show high levels of velocity distributions, namely, 20–250 mm/s, when they are lubricated with acid-based liquids or ILs. This is also in line with the surfaces of Si_3N_4 and SiO_2 under the lubrication of acid-based liquids. In liquid superlubricity, hydrodynamic effects play a critical role in separating the two contact surfaces, especially for liquids with low viscosity, but a lower velocity generally limits its contribution to achieving superlubricity. The distributions of the highest velocity are related not only to the characteristics of molecules but also to

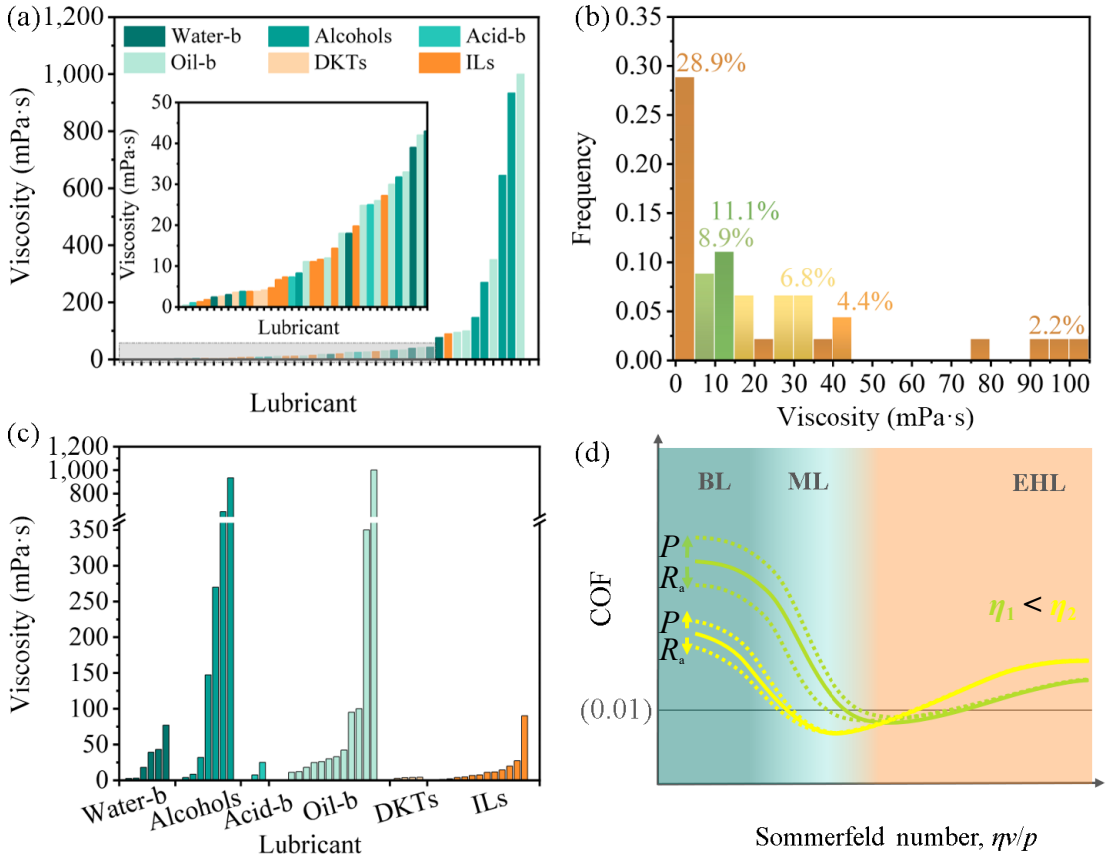

Fig. 4 (a) Viscosity distributions of superlubricating lubricants, (b) frequency distributions with a bin size of 5 mPa·s, and (c) viscosity distributions classified by lubricants in (a). (d) Classical Stribeck curve changing with surface roughness and applied contact pressure.

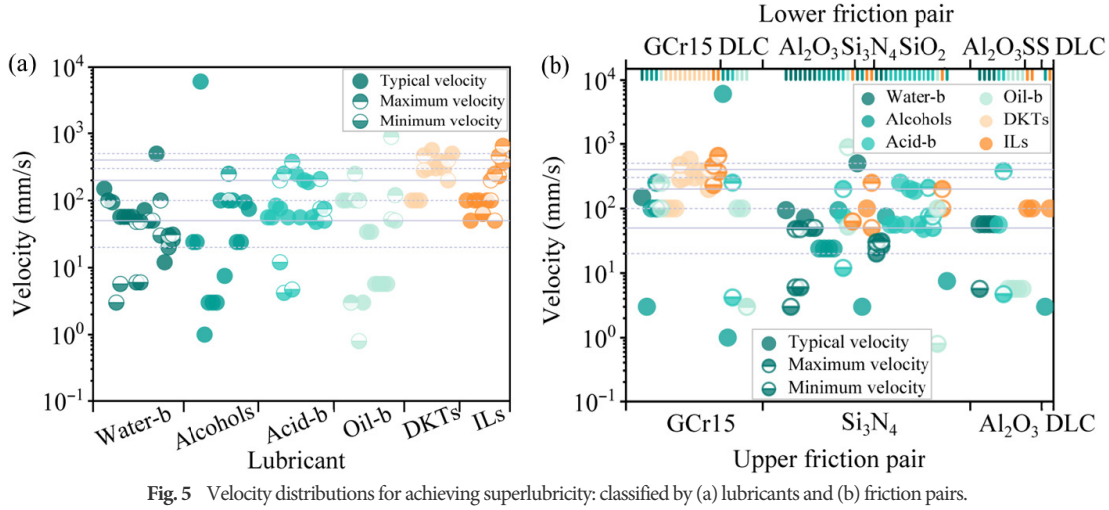

Fig. 5 Velocity distributions for achieving superlubricity: classified by (a) lubricants and (b) friction pairs.

the apparatus used in the friction test, because high speed causes vibrations, noise, and even equipment destruction. Thus, it should be noted that the distributions of the highest velocity in Fig. 5 may not be the real velocity constraints of the lubricants.

For alcohols as well as aqueous solutions containing hydration ions and acid-based lubricants, their superlubricity showed a wide velocity distribution from 3 mm/s (hydrated ions on Si_3N_4 and sapphire [71]) to 500 mm/s (glycerol on self-mated Si_3N_4 surfaces [81]). Compared with oil-based lubricants, DKTs, and ILs, a wide variety of aqueous solutions are important reasons for this wide distribution; however, most importantly, aqueous solutions achieve superlubricity at low velocities, with a significant contribution from the hydration effect. The hydrated ions are typical lubricants that achieve superlubricity at a low velocity. The divalent ($MgCl_2$, $CaCl_2$, $SrCl_2$, and $BaCl_2$) and trivalent ions ($AlCl_3$, $CeCl_3$, $CrCl_3$, $LaCl_3$, and $ScCl_3$) showed excellent lubrication performance, with COFs of 0.005–0.006 and 0.002–0.004, respectively, under a contact pressure of 250 MPa. For three trivalent ions, the velocity for achieving superlubricity could be as low as 3.1 mm/s in a boundary lubrication state. Divalent ions can reduce the surface potential and surface charge density. Trivalent ions can neutralize negatively charged surfaces and result in charge inversion owing to excess adsorption of cations, which ensures strong adsorption of hydrated multivalent ions on friction surfaces. As mentioned above, aqueous P(OEGMA) can also realize superlubricity at a low velocity of 6 mm/s, which is

predominated by hydrodynamic effects after a long time (> 1,800 s) running-in with the establishment of a boundary film [76]. The superlubricity of the glycerol aqueous solution could be obtained between sapphire and sapphire surfaces after a 450 s running-in with H_3PO_4 solution. The COF increased from 0.004 to 0.12 as the velocity changed from 57 to 2 mm/s, and the minimum velocity can reach 18 r/min (approximately 5.7 mm/s) [80]. The pure glycerol without water showed an ultralow COF of 0.004 between the steel and ta-C surfaces at a velocity as low as 3 mm/s. The mechanism is dominated by elasto-hydrodynamic lubrication with the formation of a 4.7 nm thick tribofilm. When the velocity was reduced to 1 mm/s, the COF increased to approximately 0.01 under severe boundary conditions, and the tribofilm thickness decreased to 2.3 nm [87].

In the case of acid-based lubricants, the velocity for achieving superlubricity shows higher and more concentrated distributions than those of water-based lubricants and alcohols, ranging from 50 to 250 mm/s. The typical acid-based lubricants include inorganic acids (H_3PO_4 [95, 101], HCl [93], H_3BO_3 [32], H_2SO_4 [34], etc.) and organic acids (latic acid [33], hydroxypropionic acid [92], etc.). The superlubricity of acid-based lubricants was attributed mainly to the H^+ ions and hydrogen network produced by water and acid molecules. H^+ ions lead to the formation of a smooth surface and the corresponding reduction in the contact pressure, thus facilitating the realization of hydrodynamic lubrication. The superlubricity of acid-based lubricants is achieved primarily on specific surfaces, such as Si_3N_4, SiO_2, sapphire, ruby, and glass, which is one of the important reasons for the concentrated distribution of velocity. Owing to the formation of a hydrogen network and an easy-shear layer in the running-in process, acid-based lubricants generally have relatively excellent load-bearing capacity. Its superlubricity is more sensitive to the speed than to the load condition, as shown in Figs. 6(a)–6(d). The superlubricity of H_3PO_4 solution can be obtained between sapphire and sapphire or ruby surfaces. When the rotation speed is greater than 15 r/min (4.71 mm/s), the COF remains nearly unchanged at the 0.004 level when the velocity is greater than 9.42 mm/s. A 3-hydroxyproionic acid aqueous solution ($3HPA_{aq}$) shows excellent lubrication performance for steel and a-C films. The lowest velocity can reach 4.19 mm/s, and the minimum COF of 0.0025 emerges at 50.3 mm/s [92]. The COF depends directly on the viscosity of the lubricant because of the predominant role of the hydrodynamic effect. The superlubricity of $3HPA_{aq}$ was ultimately destroyed with the continuous increase of velocity owing to the high viscosity (7.31 mPa·s after the friction test) under hydrodynamic lubrication. The real concentration of acid-based liquids increases with the evaporation of water molecules in the friction process. As shown in Figs. 6(e) and 6(f), the concentration of H_3PO_4 solution increased rapidly during the initial 300 s and remained nearly unchanged at 80 wt%, which was accompanied by a rapid increase in viscosity from ca. 1 to 25 mPa·s [95]. The above viscosity changes during the friction process also hold true for other aqueous solutions.

Oil-based lubricants generally have a high viscosity when practical lubrication is considered in engineering. This makes it difficult to exert the hydrodynamic effect. The distribution of velocity that achieves superlubricity is in the wide range of 67–300 mm/s, and the minimum velocity can be as low as ca. 1 mm/s. Silicone oil had an ultralow COF of 0.004 between the Si_3N_4 and glass surfaces after a running-in with acid solution, and the velocity could be reduced to an extremely low value of 0.8 mm/s [12]. The tribochemical reaction in the running-in period leads to a reduction in the COF under mixed lubrication, but it has no evident influence on the COF under hydrodynamic lubrication. The dependence of the COF and viscosity demonstrated the predominant role of hydrodynamic lubrication in achieving the superlubricity of silicone oil, as shown in Figs. 7(a) and 7(b). With increasing viscosity of silicone oil from 100 through 350 to 1,000 mPa·s, the COF at higher rotation speeds increased because of the dominant role of hydrodynamic lubrication, while those at lower rotation speeds decreased because of the dominant role of mixed lubrication. When the viscosity of silicone oil was 1,000 mPa·s, the minimum rotation speed for achieving superlubricity decreased to 2 r/min (0.8 mm/s). Long et al. [111] studied the ultralow friction performance of RA, OA, castor oil (CO), and linoleic acid (LA) between steel and a-C or ta-C coatings. Tribological tests are performed using a linear reciprocating tribometer with a pin-on-flat configuration, and the velocity follows a sine function with a maximum value of 3 mm/s. The final roughness of mating pairs is less than 10 nm, and the

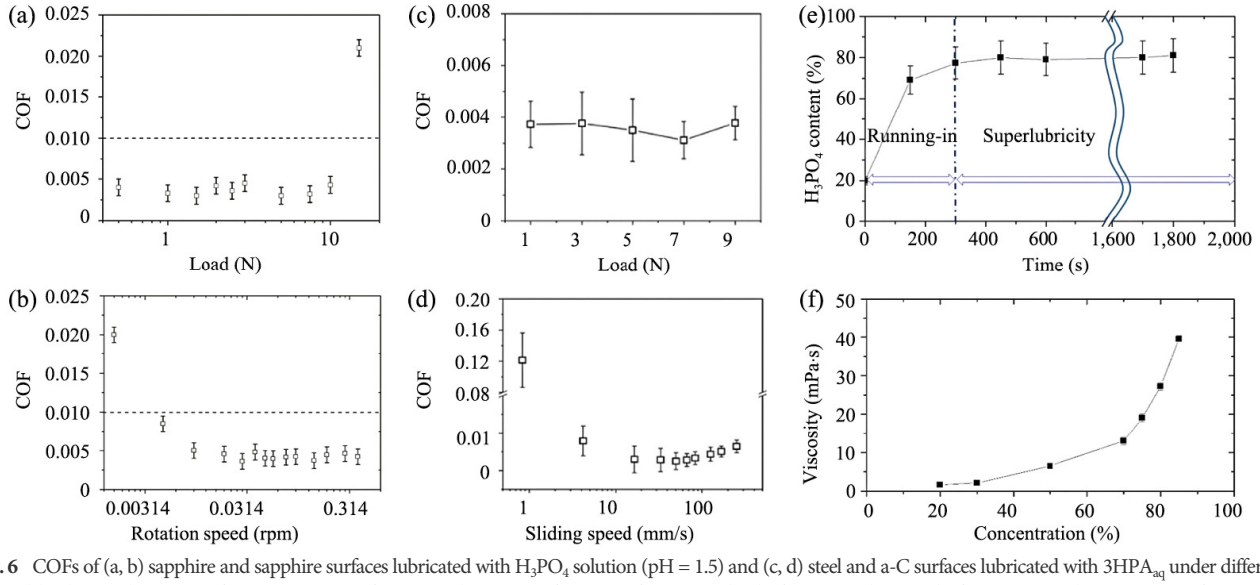

Fig. 6 COFs of (a, b) sapphire and sapphire surfaces lubricated with H_3PO_4 solution (pH = 1.5) and (c, d) steel and a-C surfaces lubricated with $3HPA_{aq}$ under different normal loads or velocities. (e, f) Concentration of H_3PO_4 solution as a function of time at a load of 1.5 N and a speed of 76 mm/s and viscosity as a function of concentration. Reproduced with permission from Ref. [101] for (a, b), © The author(s) 2014; Ref. [92] for (c, d), © Elsevier Ltd. 2022; Ref. [95] for (e, f), © The author(s) 2014.

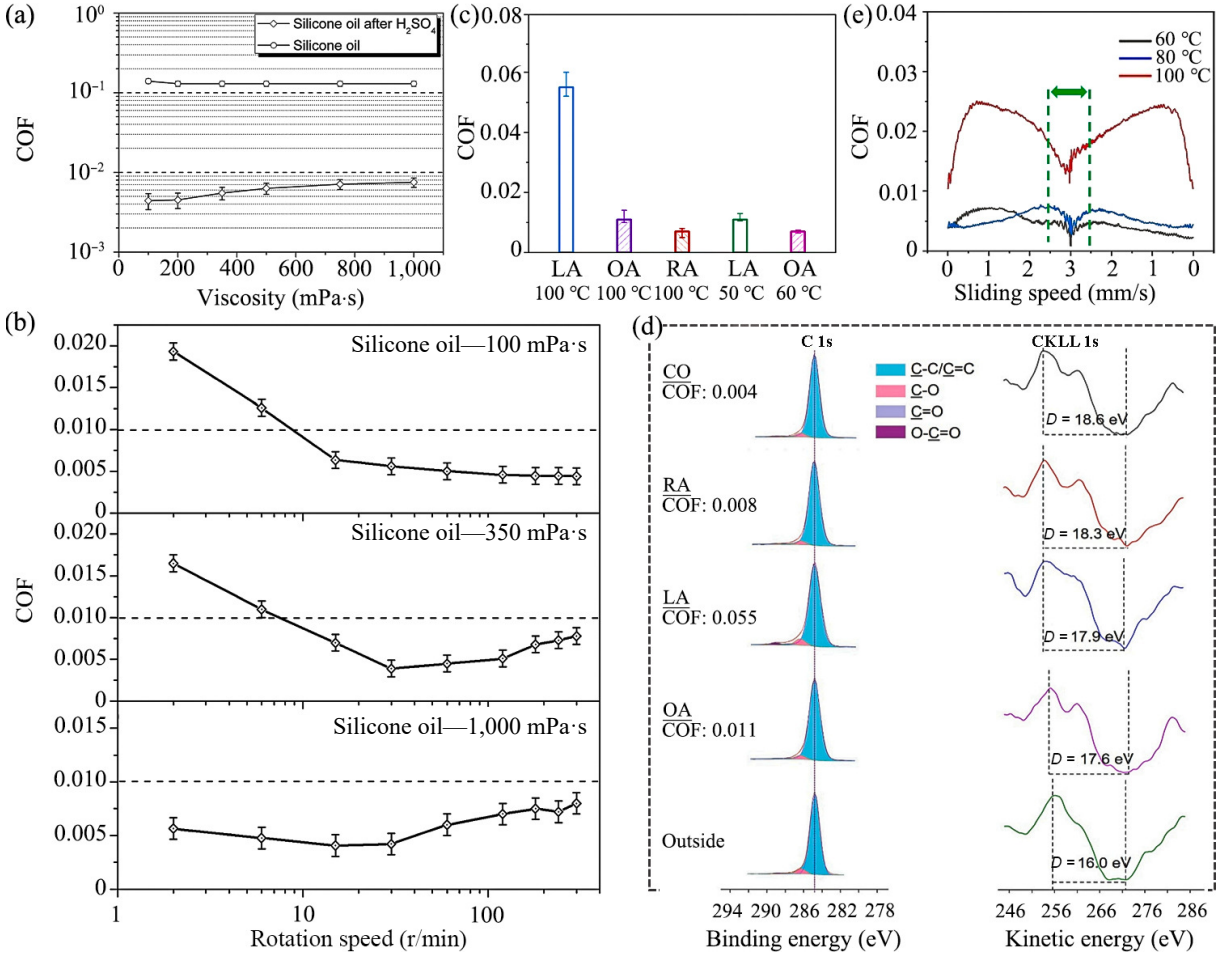

Fig. 7 (a, b) Superlubricity of silicone oil between Si_3N_4 and glass after running-in with H_2SO_4 solution. (c) Different temperatures were used to ensure the same viscosity (11 mPa·s) and tribofilm thickness of approximately 3 nm, and (d) corresponding C 1s XPS spectra and first derivation of X-ray-excited auger electron spectroscopy (XAES) CKLL spectra of a-C wear scars after friction tests. (e) Correlation between COF and sliding speed obtained between steel and Si_3N_4 under boundary lubrication by RA. Reproduced with permission from Ref. [12] for (a, b), © The Royal Society of Chemistry 2015; Ref. [111] for (c, d), © Elsevier Ltd. 2022; Ref. [105] for (e), © Elsevier Ltd. 2022.

lambda ratio stays far below unity, indicating that their lubrication is under boundary lubrication. The lubrication properties followed the trend of CO (μ = 0.004) < RA (μ = 0.008) < OA (μ = 0.011) << LA (μ = 0.055) between the steel and a-C surfaces at 100 °C. The better performance of CO was partially related to its greater viscosity (18 mPa·s for CO, 11.1 mPa·s for RA, 5.0 mPa·s for OA, and 3.3 mPa·s for LA) and capacity to form a thicker lubrication film of approximately 5 nm. For RA lubrication, when the temperature decreased from 100, 80 to 60 °C, the viscosity decreased from 11.1, 24.8 to 42.0 mPa·s, and the corresponding COFs were 0.014, 0.005, and 0.004 between the steel and Si_3N_4 surfaces (Fig. 7(c)) [105]. This can also be explained by the improvement in lubrication performance via a decrease in the temperature of LA and OA, as shown in Fig. 7(e). High viscosity generally means a high load support capacity, which is conducive to avoiding the direct contact of friction pairs, particularly boundary lubrication, when the hydrodynamic effect is negligible. The superlubricity of oil-based liquids could be achieved by reducing the temperature and thereby increasing the viscosity, which is feasible under low-velocity conditions but not suitable for high-velocity conditions. Under high-velocity conditions, lubrication is affected by the hydrodynamic effect, and thus, a low viscosity is needed. The detailed mechanism of ILs will be revealed latter. In addition, the realization of superlubricity is limited by high speeds. Under the dual induction of mechanical shear and friction heat, unsaturated oil-based molecules are more prone to decomposition failure. CO exhibits superlubricity on Nitinol 60 alloys [112]. The high polarity and long chains of CO molecules cause OH-terminated surfaces via dissociation under boundary lubrication. The sliding speed has a more severe influence on the tribological behavior of the Nitinol 60 alloy under CO lubrication than that of load because of the characteristic structure of CO, and the superlubricity is destroyed with increasing sliding speed at the stable stage. A high sliding speed causes the temperature to increase, which generally results in the oxidation of CO and a decrease in viscosity.

For DKTs, the velocity for achieving superlubricity ranges from 200 to 500 mm/s, and the minimum velocity can reach 100 mm/s under some conditions. The superlubricity of particular 1,3-diketone was achieved between GCr15 self-mated parts at 100 mm/s using SRV [107]. The achievement of superlubricity experienced 8 h of running-in, at which time the tribochemical polishing reaction caused conformal and smooth surfaces. A transition from boundary lubrication to fluid lubrication occurred, and the lower dynamic viscosity of approximately 2.6–3.6 mPa·s (90 °C) should be responsible for its underperformance at boundary states. Through molecular dynamic simulations, it was elucidated that mechanical shearing induced the orientation of molecules in the friction gap, and the effective viscosity in the sliding direction was reduced so that thin film lubrication could

take place [107]. Ethylacetophenone (EAP) solutions with different benzoylacetone (BZA) contents show ultralow friction on steel surfaces, and their friction behavior is significantly sensitive to the BZA content and velocity conditions [122]. The superlubricity can be realized only when the BZA content is 50% at a narrow velocity ranging from 502 to 565 mm/s and loads between 2 and 3 N, as shown in Figs. 8(a) and 8(b). The lubrication in the mixed state was affected by both the hydrodynamic effect and the asperity contact. Moreover, as shown in Figs. 8(d) and 8(e), compared with traditional lubricant PAO, DKTs showed an abnormal friction behavior that deviated from that of the classical Stribeck theory, which showed an extremely low COF with increasing velocity. As non-Newtonian fluids, they have strong intermolecular forces and experience evident shear-thinning behavior. DKTs can adjust their viscosity autonomously to adapt to different velocities. As shown in Fig. 8(c), the viscosity of PAO essentially remains unchanged at 7 mPa s when the shear rate varies from 0.1 to 1,000 s^{-1}, while that of diketone (1-(4-ethyl phenyl) butane-1,3-dione, EPBD) decreases from 70 to 4 mPa·s. This discrepancy is related to the molecular alignment of the ellipsoid molecular structure of DKTs as liquid crystals, which is likely to result in thin film lubrication rather than hydrodynamic lubrication.

In the case of ILs, the velocity for achieving superlubricity ranges at a relatively low level between 50 and 250 mm/s compared with that of DKTs. The adsorption and shear properties of ILs are controlled jointly by cations and anions. The PILs based on FA, PA, IA, or TA showed excellent lubrication performance at the GCr15 surface [123]. Among them, FA-ILs had the lowest COF, and superlubricity appeared when the rotating speed reached 600 r/min or the temperature reached 75 °C, as shown in Figs. 9(a) and 9(b). A high velocity ensured the hydrodynamic effects at frictional surfaces. The lubricity is affected by viscosity, indicating that the system is under mixed lubrication rather than boundary lubrication. The influence of temperature on friction behavior is ascribed to the decrease in viscosity from ca. 20 to 0.4 mPa·s. High viscosity at low temperatures provides great load-bearing capacity to resist the direct contact of friction pairs, but it also shifts the lubrication to the hydrodynamic regime and leads to a large COF for high internal shear. The aqueous solutions of ILs also showed similar velocity constraints. The $[Li(EG)]PF_{6(aq)}$ prepared from lithium hexafluorophosphate ($LiPF_6$) and ethylene glycol (EG) exhibited excellent superlubricity at Si_3N_4 self-mated interfaces over a wide range of 50–250 mm/s, as shown in Figs. 9(c) and 9(d) [126]. Li(EG)]PF6 has a high viscosity of 20.1 mPa·s, but the viscosity of its aqueous solution is as low as 1.3 mPa·s. The low viscosity deteriorates the load-carrying capacity of $[Li(EG)]PF_{6(aq)}$, resulting in high sensitivity to load conditions; however, the low viscosity also reduces the shearing resistance and facilitates ultralow friction. The lowest COF of 0.0033 was observed for mixed lubrication (λ = 1.8) when the velocity was 100 mm/s. 1-Ethyl-3-methylimidazolium trifluoromethane sulfonate ([EMIM]TFS) showed stable superlubricity (μ < 0.01) with water at the Si_3N_4 and SiO_2 surfaces in mixed lubrication, and this ultralow friction failed when the velocity was less than 50 mm/s or greater than 250 mm/s [127]. The constraints at high velocity are related to the high internal shear resistance of $[EMIM]TFS_{(aq)}$, as depicted in Figs. 9(e) and 9(f). The superlubricity failure occurred when the viscosity reached 3.4 mPa s. The superlubricity of ILs or their aqueous solutions is typically in mixed or hydrodynamic regimes. The influence of velocity on the superlubricity of ILs depends on the hydrodynamic effect; thus, the viscosity of the lubricant needs to be in the appropriate range to achieve superlubricity.

3.4 Long running-in period and severe wear loss

A long running-in period is a common practice for most liquid superlubrication systems before the occurrence of superlubricity. Running-in causes a smoother surface (R_a < 10 nm) and perfect conformity of two contact surfaces at the asperity level, but it is accompanied by unexpected severe wear loss and contact pressure reduction. Owing to the long-time running-in, the concept of ultralow wear is rarely mentioned in the study of liquid superlubricity, because the running-in process and ultra-low wear

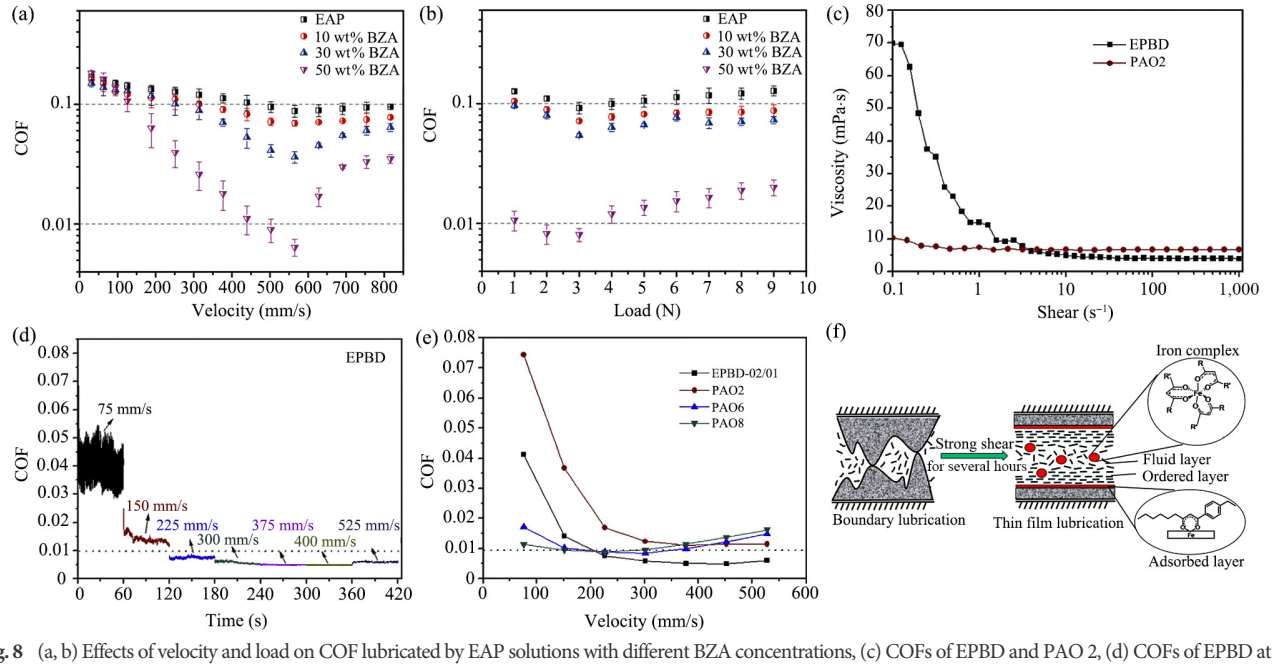

Fig. 8 (a, b) Effects of velocity and load on COF lubricated by EAP solutions with different BZA concentrations, (c) COFs of EPBD and PAO 2, (d) COFs of EPBD at 7-speed ramps, and (e) average COFs of EPBD, PAO 2, PAO 6 and PAO 8 on worn surfaces after friction test using EPBD. (f) Schematic diagram of the lubrication mechanism of 1,3-diketones on steel surfaces. Reproduced with permission from Ref. [122] for (a, b), © The Royal Society of Chemistry 2018; Ref. [117] for (c–e), © Elsevier Ltd. 2018; Ref. [107] for (f), © American Chemical Society 2015.

rate seem to be contradictory, which is significantly different from the solid superlubricity. The running-in period is affected by multiple factors, such as the materials of friction pairs, types of lubricants and tribological conditions (e.g., velocity, load, temperature, humidity, and atmosphere). As shown in Fig. 10(a), water-based lubricants commonly show superlubricity on the Si_3N_4, SiO_2, and sapphire surfaces. Their running-in periods change with the different configurations of lubricating additives and tribological conditions. In specific cases, the running-in period can be eliminated to an ultrashort phase, which is similar to the lubrication of oil-based lubricants and ILs. However, the long running-in period of DKTs is still an unresolved problem, and it changes from 5,400 to 28,800 s. For different materials of friction pairs, as shown in Fig. 10(b), GCr15 self-mated friction pairs show superlubricity due to the lubrication of DKTs or oil-based lubricants, but the extremely long running-in period, even up to 8 h for DKTs, is always difficult to eliminate [107]. When GCr15 is replaced by DLC coatings (e.g., GCr15 and DLC surfaces, DLC and DLC surfaces), these interfaces can establish superlubricity after a short running-in period, and the effective lubricants include OA, CO, and elaidic acid. GCr15 self-mated surfaces show a short running-in period of approximately 750 s because of the lubrication of the aqueous IL solution [131] or even without a running-in period (herein, the duration is artificially set to 1 s in a logarithmic coordinate system) because of the lubrication of pure ILs [123]. The Si_3N_4 surfaces mated with Al_2O_3, SiO_2, and Si_3N_4 need to experience a running-in period of approximately 10 min when they are lubricated with water-based lubricants or alcohols. The running-in period could be eliminated by the introduction of hydrated ions into solutions. When they are lubricated with oil-based lubricants, pre-running-in treatments with acid solutions or alcohol solutions should be adopted before superlubricity is achieved.

The running-in period-induced wear loss is unpredictable. Severe wear loss usually occurs at the very beginning of the running-in period, and once superlubricity is achieved, the wear

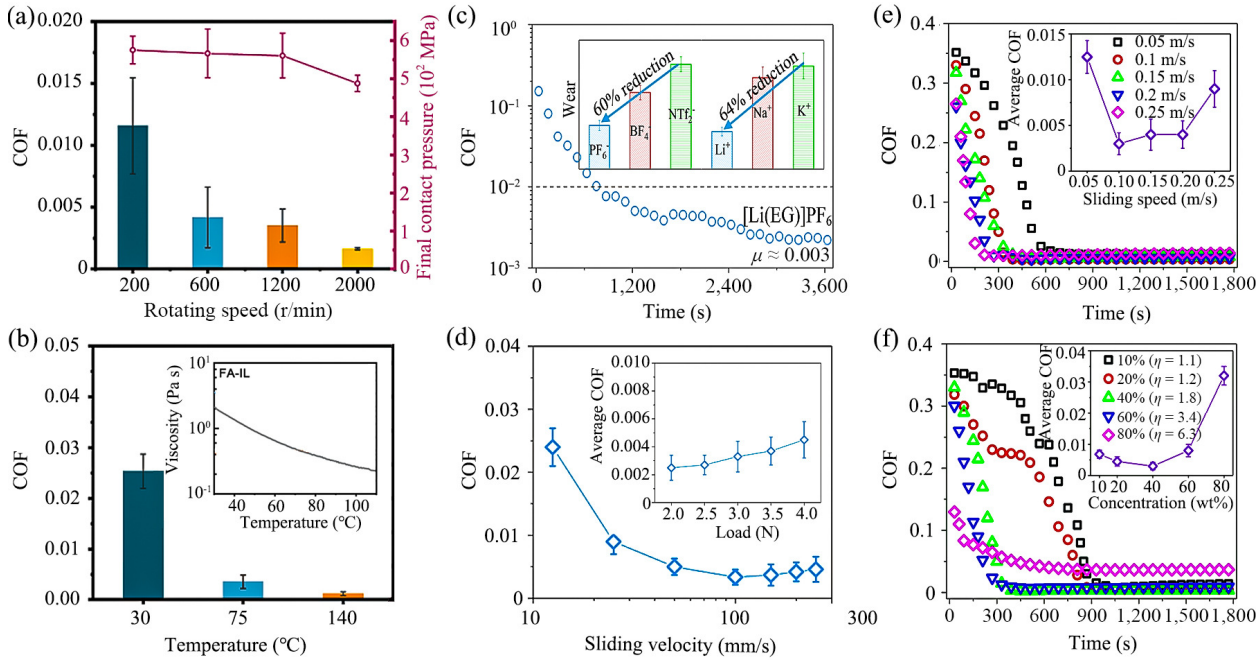

Fig. 9 (a, b) COFs of FA-ILs with various speeds (T = 75 °C) and temperatures (v = 1,200 r/min). The inset shows viscosity of FA-ILs. (c, d) Friction behavior of ILs prepared with monovalent metal salts and EG and changes in COF of [Li(EG)]$PF6_{(aq)}$ with velocity and load between Si_3N_4 self-mated interfaces. (e, f) COFs of Si_3N_4 and SiO_2 pairs lubricated with 40 wt% [EMIM]$TFS_{(aq)}$ at different speeds or lubricated with different concentrations of [EMIM]$TFS_{(aq)}$. Reproduced with permission from Ref. [123] for (a, b), © Elsevier Ltd. 2023; Ref. [126] for (c, d), © American Chemical Society 2019; Ref. [127] for (e, f), © American Chemical Society 2018.

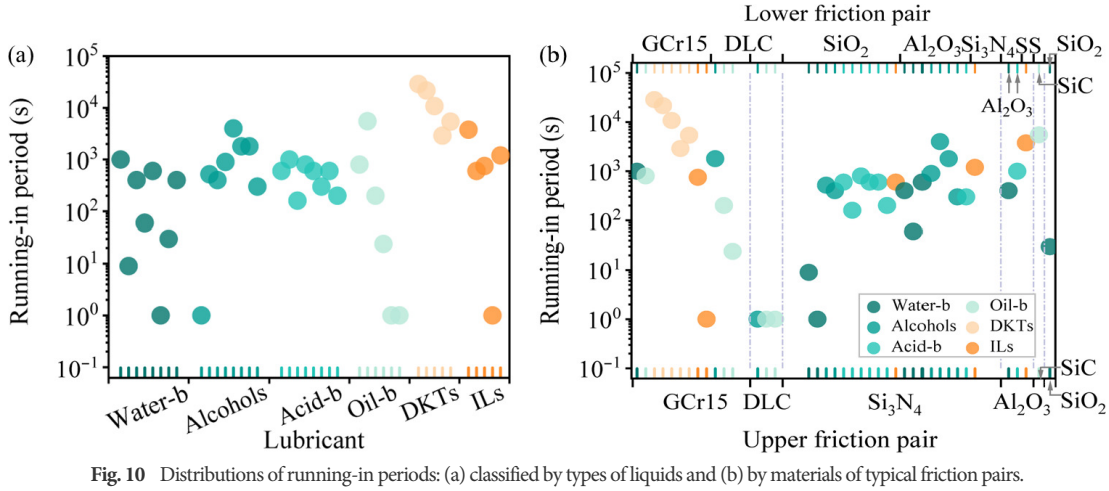

Fig. 10 Distributions of running-in periods: (a) classified by types of liquids and (b) by materials of typical friction pairs.

loss approximates zero, which is considered atom-by-atom wear [41, 89], as depicted in Fig. 10(a). Under the lubrication of phosphoric acid solution, the superlubricity of sapphire against ruby (or against itself) results in a wear scar with a diameter of 200 μm. The wear rates are as low as 2.67×10^{-10} and 1.9×10^{-9} mm³/(N·m), respectively. Figure 11(c) shows the corresponding COF curve of sapphire against ruby, and the running-in period is approximately 320 s. Since wear loss occurs at extremely short initial time, the wear volume remains constant, while the wear rate decreases as the superlubricity progresses; however, in reality, a smaller amount of wear, rather than an apparent ultralow wear rate, should be expected. The interface of Si_3N_4 ball and SiO_2 disk lubricated with the IL aqueous solution shows a running-in period of 600 s and a total wear rate of 5.2×10^{-7} mm³/(N·m) [127]. However, the corresponding diameter of the wear scar reaches 321 μm, and the contact pressure decreases from approximately 700 to 30 MPa. The mixtures of hydrated ions and PEG solutions show excellent lubrication performance between Si_3N_4 and sapphire with a running-in period of less than 60 s. The FCP reaches 555 MPa, and an ultralow wear rate of 1.9×10^{-9} mm³/(N·m) (the corresponding diameter of wear scar is 110 μm) is obtained [141]. The synergistic action of hydration and hydrodynamic lubrication is responsible for these outstanding lubrication properties. In addition, the solution of PEG and tannic acid also shows an ultrashort running-in period of 9 s between the Si_3N_4 and glass surfaces, and the FCP reaches 410 MPa. The wear rate of the glass is 1.2×10^{-8} mm³/(N·m) over a sliding distance of 30 m. The friction pairs of Al_2O_3 and dual-phase TiB_2–MoS_2 film lubricated by PAO 10 exhibit superdurable superlubricity characterized by an ultralow COF of 0.007 and a wear rate of 10^{-9} mm³/(N·m) over an unprecedentedly long sliding distance of 12.6 km (ca. 70 h), while the running-in period is up to ca. 7 h [106]. The TiB_2–MoS_2 film catalytically activated the decomposition of oil molecules, thus leading to the operando formation of fullerene-like carbon, which provides a promising strategy to develop high-performance superlubricating materials that meet stringent conditions for demanding applications.

Specifically, given different types of lubricants, aqueous solutions show a relatively short period of running-in compared with non-aqueous solutions (e.g., oil-based lubricants and DKTs). The running-in period of aqueous solutions can be successfully eliminated by adding hydrated ions or changing the pH value. Hydrated ions not only play an important role in achieving superlubricity but also facilitate the shortening of the running-in period, particularly in aqueous solutions containing PEG, as depicted in Figs. 12(a) and 12(b) [148]. Additionally, in the current systems, the running-in period increased with increasing viscosity of KCl and PEG mixtures but did not affect the final COF. The low pH is related to the high reactivity of the liquid environment, which also greatly contributes to shortening the running-in period (Fig. 12(c)) [34]. Moreover, the appropriate content of lubricant determines either the degree of superlubricity or the duration of the running-in process. The P(OEGMA) aqueous solution shows an ultralow COF of less than 0.01 when its concentration changes from 20 to 60 wt% and has a shorter duration of running-in but in a narrower range of concentrations from 40 to 60 wt% [76]. The running-in period is also affected by the tribological conditions, such as velocity, load, temperature, and humidity. The effects of load and velocity depend on the lubrication regime. The low load and high velocity, namely, a high Sommerfeld number, generally tend to be in a hydrodynamic lubrication state that reduces or even avoids the direct contact of frictional pairs. This is not set in stone because the hydrodynamic

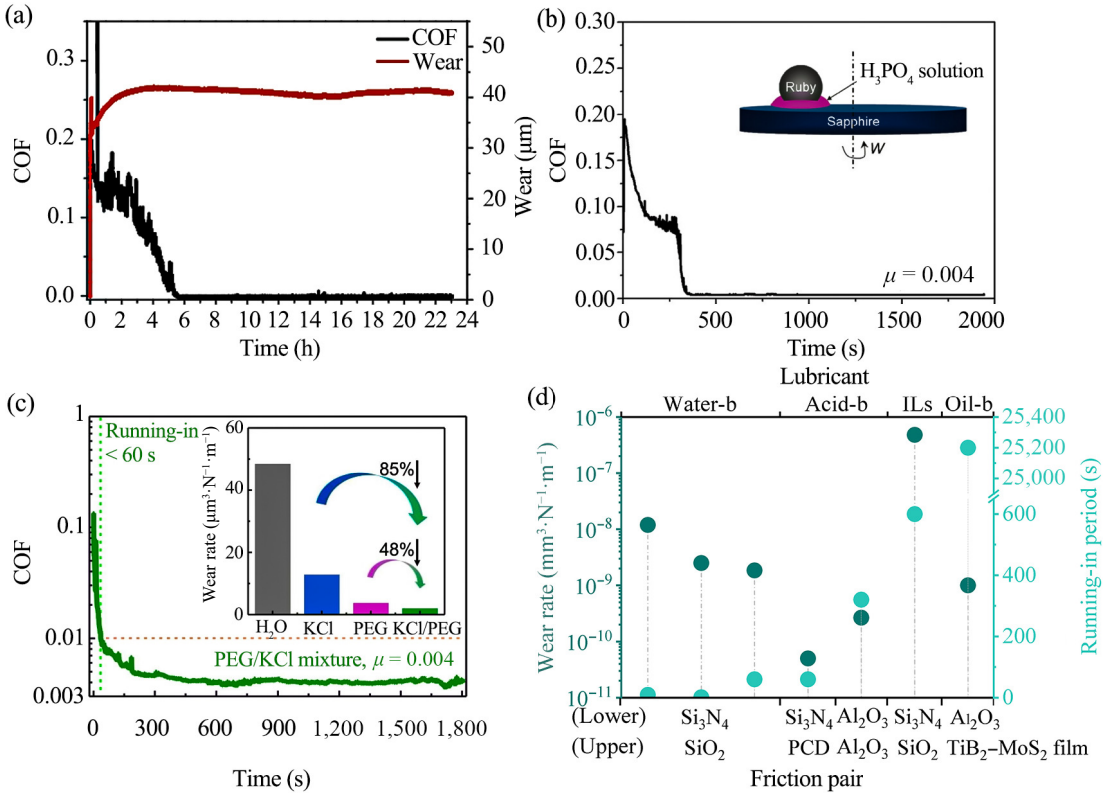

Fig. 11 (a) Typical dependence of COF and wear loss of 100Cr6 self-mated pairs lubricated with DKTs. (b) COFs of H_3PO_4 solution lubricant (pH = 1.5). (c) COFs of PEG/KCl mixture between Si_3N_4 and sapphire surfaces and corresponding wear rate. (d) Statistics of running-in period and wear rate. Reproduced with permission from Ref. [41] for (a), © Springer Science Business Media, LLC 2009; Ref. [101] for (b), © The author(s) 2014; Ref. [148] for (c), © Elsevier Inc. 2020.

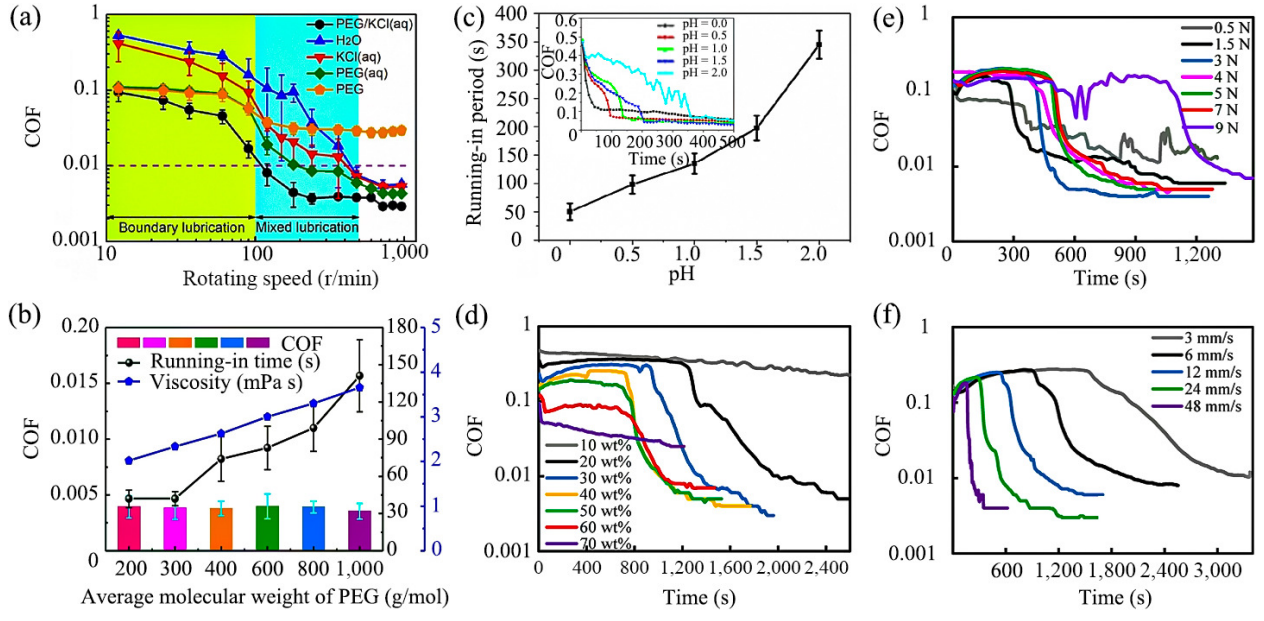

Fig. 12 (a, b) Superlubricity obtained with mixtures of hydrated ions and PEG solutions between Si_3N_4 and sapphire surfaces; COF and viscosities for mixed solutions of KCl and PEG with different average molecular masses. (c) Effects of pH on running-in period and superlubricity of Si_3N_4 and glass surfaces lubricated with H_2SO_4 solution. (d–f) Influence of concentration, load, and velocity on running-in period of Si_3N_4 and Al_2O_3 surfaces lubricated with P(OEGMA) solution. Reproduced with permission from Ref. [148] for (a, b), © Elsevier Inc. 2020; Ref. [34] for (c), © American Chemical Society 2012; Ref. [76] for (d–f), © American Chemical Society 2019.

lubrication results in insufficient running-in, and a longer period of running-in is needed before achieving superlubricity. The load and speed have different effects on the frictional behavior of the system in terms of lubrication state. The P(OEGMA) aqueous solution had short running-in time when the load varied between 3 and 7 N, but both the lower and higher loads could result in long running-in time or even superlubricity failure due to insufficient running-in or excessive wear, respectively. A high velocity seems to be helpful for reducing the running-in period of the P(OEGMA) aqueous solution, as shown in Fig. 12(f). The running-in period is affected by numerous factors, but how to eliminate their influence is still an unresolved scientific problem. Herein, the main approaches are summarized as follows: pre-running-in under special tribological conditions, pre-running-in with different lubricants, and regulating environmental conditions.

(1) Pre-running-in under specific tribological conditions

Friction behavior is determined by the surface structure of two friction pairs, such as roughness and chemical state. Liquid superlubricity is initially achieved on the surface of mica sheets with atomic smoothness. Some studies have achieved liquid superlubricity with industrial-grade roughness surfaces, but generally, a surface roughness of less than 10 nm is considered necessary to achieve liquid superlubricity. At the macroscale, surface roughness determines the lubrication states of friction pairs from the perspective of the classical Stribeck theory. The lower the roughness is, the easier it is to achieve mixed and hydrodynamic lubrication, thus reducing the dependence of lubrication on the surface roughness. The smooth surface also means an increase in the real contact area and a subsequent decrease in the contact pressure. At the microscale, a reduction in surface roughness improves the contribution of short-range surface forces and facilitates the achievement of superlubricity at low speed [149]. Pretreatment via a pre-running-in process under specific load or velocity conditions is an effective method to promote stable superlubricity. As shown in Figs. 13(a) and 13(b), in contrast to the conditions for achieving superlubricity, boundary lubrication and mixed lubrication at high load or low speed are adopted in the pretreatment. The superlubricity of the H_3PO_4 solution between Si_3N_4 and glass could be achieved at 125 mm/s after the running-in process at a low velocity of 42 mm/s, but it failed after the running-in process at a high velocity of 628 mm/s [99]. High velocity results in more friction heat and excessive moisture loss, which is the most important reason for lubrication failure. This holds true for other aqueous lubricants. Moreover, high speed leads to an insufficient running-in process and restricts the formation of a strong lubrication film that can resist wear damage at medium velocities. Conversely, the running-in process at lower velocities improves surface reactivity and results in both enhanced hydration and hydrodynamic effects, thus facilitating the achievement of superlubricity [24]. For the DKTs reported by Du et al. [119] (Fig. 13(c)), the superlubricity could be obtained at 1 N and 377.0 mm/s after 5 min of running-in at the same load but at a lower speed of 62.8 mm/s. The achievement of superlubricity can be divided into three stages, pre-running-in, tribological reactions and stable superlubricity. In addition to the reduction in contact pressure, the running-in exposes the nascent matrix to the frictional interfaces, thus motivating the subsequent tribological reactions that occur primarily at the second stage. Remarkably, pre-running-in could generally eliminate the secondary running-in period at the superlubricity stage, but this seems not to be true for the lubrication of DKTs. Certainly, the superlubricity can also be obtained after pre-running-in without changing the velocity conditions, as shown in the insert in Fig. 13(f). CPSO shows superlubricity on Si_3N_4 and sapphire surfaces at 190 °C, 6 N, and 300 r/min after 10 min pre-running-in with H_3PO_4 solutions at 25 °C, 10 N, and the same velocity. The pre-running-in with specific lubricants aims to form a tribochemical layer, which will be depicted in the following section.

(2) Pre-running-in with specific lubricants

Pre-running-in with specific lubricants, such as acid or PEG solutions, is another effective method to shorten the running-in period. The superlubricity of alkali metal ions (Li^+, Na^+, K^+) could

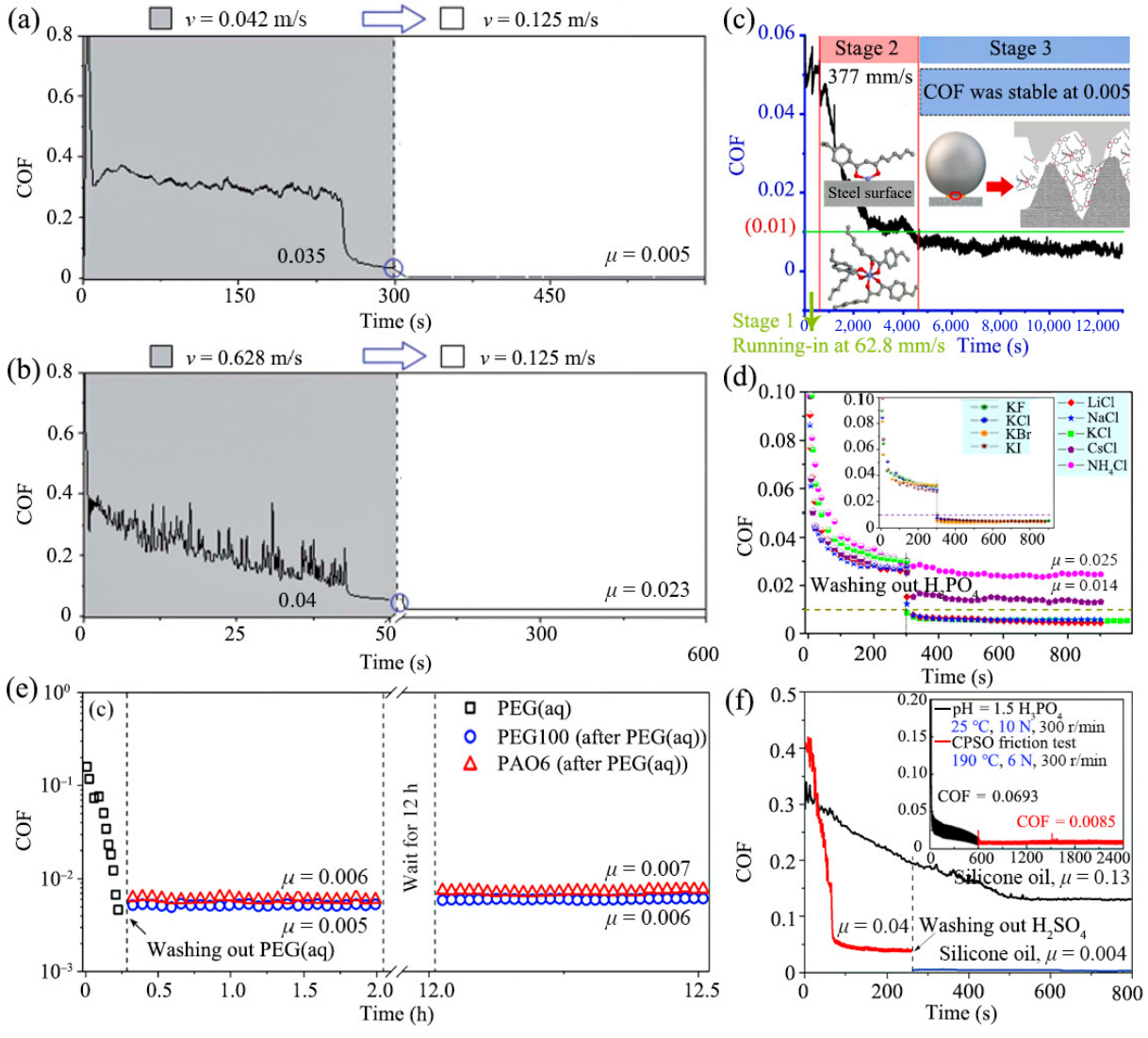

Fig. 13 Pre-running-in with specific tribological conditions or with specific lubricants. (a, b) Pretreatment of Si_3N_4 and glass surfaces with specific velocity conditions under the lubrication of H_3PO_4 solution. (c) Superlubricity of 0206-Fe(60%) obtained with multistage treatments. (d) Superlubricity of hydrated alkali metal ions on Si_3N_4 and sapphire surfaces achieved after pre-running-in with H_3PO_4 solution. (e) Superlubricity of PAG and PAO achieved after pre-running-in with PEG solution. (f) Superlubricity of silicone oil between Si_3N_4 and glass surfaces obtained by pre-running-in with H_2SO_4 solution. The inset shows superlubricity of CPSO by pre-running-in under specific tribological conditions with acid solution. Reproduced with permission from Ref. [99] for (a, b), © The Royal Society of Chemistry 2017; Ref. [119] for (c), © Elsevier Ltd. 2022; Ref. [70] for (d), © American Chemical Society 2018; Ref. [85] for (e), © The author(s) 2018; Ref. [12] for (f), © The Royal Society of Chemistry 2015; Ref. [104] for the inset of (f), © American Chemical Society 2022.

be obtained between the Si_3N_4 and sapphire surfaces after 300 s of running-in with acid solutions (H_3PO_4, HCl, H_2SO_4, pH = 0.5–3.0), as shown in Fig. 13(d) [70]. The same method is also applicable to aqueous solutions consisting of PVA and NaCl, which show extreme-pressure superlubricity on Si_3N_4 and sapphire surfaces after 300 s of running-in with H_3PO_4 solution [69]. The pretreatment method with an acid solution is applicable to the lubrication of alcohol-based aqueous and even oil-based lubricants (e.g., silicone oil, Figs. 13(a), 13(b), and 13(f)) on the surfaces, such as Si_3N_4, SiO_2, glass, and sapphire surfaces. In addition to reducing the surface roughness and contact pressure, the application of pre-running-in with acid solutions results in the formation of a negatively charged silica layer. This silica layer traps hydrated alkali metal ions and provides excellent hydration lubrication. Aqueous PEG is also an effective lubricant for pre-running-in [85]. The surfaces of the polar molecules PAG and the nonpolar molecule PAO were robustly superior to the surfaces of GCr15 and GCr15 when pre-running-in with a 33 wt% PEG solution. Unlike the pretreatment of ceramics with acid, the treatment with aqueous PEG needs to be continued until the superlubricity state emerges, after which it is maintained for a few minutes. With the improvement in surface roughness and reduction in contact pressure, the running-in with PEG solution also leads to the formation of a tribochemical layer containing iron oxides, FeOOH, $Fe(OH)_3$, and other oxygen-containing components as an effective boundary lubricant. Notably, this easier shearing layer formed by PEG remained on the steel surfaces, and no further tribochemical reactions occurred between PAG or PAO and steel surfaces.

(3) Regulating environmental conditions

The environmental conditions, including temperature, atmosphere, and humidity, not only play important roles in achieving superlubricity but also affect the running-in period [79, 150, 151]. The influence of temperature on running-in is mainly linked to changes in tribological reactivity and viscosity. Figure 14(a) shows that the long running-in period (6,000 s) of

PILs (2,5-furandicarboxylic acid (FA-IL)) on steel surfaces could be eliminated when the temperature reached 75 °C [123]. The resulting decrease in viscosity improved the adsorption rates on the frictional surfaces. However, temperature has a converse influence on the running-in period of Si_3N_4 self-mated surfaces when lubricated with glycerol aqueous solutions, and the increased temperature increases the running-in time [81]. The oxygen content (in the surrounding environment) clearly influenced the lubrication performance of the diketone solution between GCr15 and GCr15 surfaces. The increased oxygen content from 0.3% to 50% not only shortens the initial running-in period but also reduces the COF of superlubricity, as shown in Fig. 14(b) [121]. The results demonstrate that more severe oxidation wear is activated at high oxygen contents, thus facilitating surface smoothening and contact pressure reduction. Moreover, a high oxygen content promotes the formation of chelates, which act as effective lubricants to reduce the interface resistance. Nevertheless, in some cases, the absence of oxygen can alter chemical reaction paths and lead to different friction reduction behaviors. When SiC surfaces are lubricated with isooctane, the wear debris in dry air is composed of powder-like silica particles, but that in N_2 has a high concentration of free carbon and no significant amount of elementary silicon. In the absence of oxygen and H_2O, the highly reactive nascent surfaces need to be saturated *in situ* to reach a stable state; thus, isooctane decomposition is promoted by the dangling bonds of the nascent surface under normal load and mechanical shear, as evidenced by Figs. 14(c)–14(f).

The influence of humidity on superlubricity remains elusive, and it changes with the type of liquid lubricant or frictional surface material. It seems that a humid atmosphere (45%±2% RH) is adverse to the superlubricity of isooctane on self-mated SiC [152]. In a humid atmosphere, the COF shows dramatic fluctuations in the running-in process when the reciprocating frequency is 20 Hz, with its COF varying between 0.25 and 0.65, and a minimum COF value of 0.0025 appears after approximately 1,000 m (ca. 5,500 s) of sliding distance. The humid air even leads to the failure of superlubricity when the reciprocating frequency is decreased to 2.5 Hz. Even though the SiC surfaces are completely submerged in isooctane and the maximum solubility of water molecules in the isooctane is only 110 ppm [153], the humidity still has a non-negligible influence on ongoing processes. The active water molecules partially "hydroxylated" the siloxane groups into silanol groups [154, 155]. The surfaces with silanol groups tend to sinter together in the friction process, leading to the agglomeration of wear particles. The sticky effect is the reason for the fluctuations in the COF in humid environments. The humid atmosphere results in a high COF, but it also leads to a more stable and lower COF once superlubricity is established. This is applicable to the superlubricity of both glycerol solutions (Fig. 14(g)) [79], nanodiamond glycerol colloidal solutions [150], and ILs mixed with glycerol aqueous solutions (Fig. 14(h)) [79]. For aqueous lubricants, a hydrated water layer adsorbed on surfaces is necessary for achieving superlubricity, but a lower humidity vaporizes water and deteriorates the establishment of this hydrated water layer. The firm hydrogen-bonded layer can also recover from excrescent water as long as the environment humidity is suitable, which plays an important role in controlling the superlubricity via the environment humidity.

4 Conclusions and outlook

Liquid superlubricity presents the most potential engineering application prospects, as it is similar to traditional engineering and industrial lubrication [156–158]. Compared with solid superlubric materials, they rarely suffer from environmental limitations [159, 160]. However, there is a particularly serious gap between the conditions under which liquid superlubricity has been achieved in the laboratory and those associated with practical applications. Figure 15 shows a schematic diagram of the liquid superlubricity mechanism and methods for accelerating superlubricity. Liquid superlubricity can be realized in systems that exhibit the following features: (I) smooth surface, (II) low viscosity, (III) appropriate contact pressure and velocity conditions, and (IV) reasonable liquid molecules and frictional materials. Suitable humidity and temperature conditions are also necessary, even if the liquid superlubricity is relatively less affected by the environment. To date, many efforts have addressed the first two requirements through intensive research on ultra-smooth surfaces (R_a < 10 nm) and low-viscosity liquids. The development of liquid superlubricity beyond the laboratory requires revising the

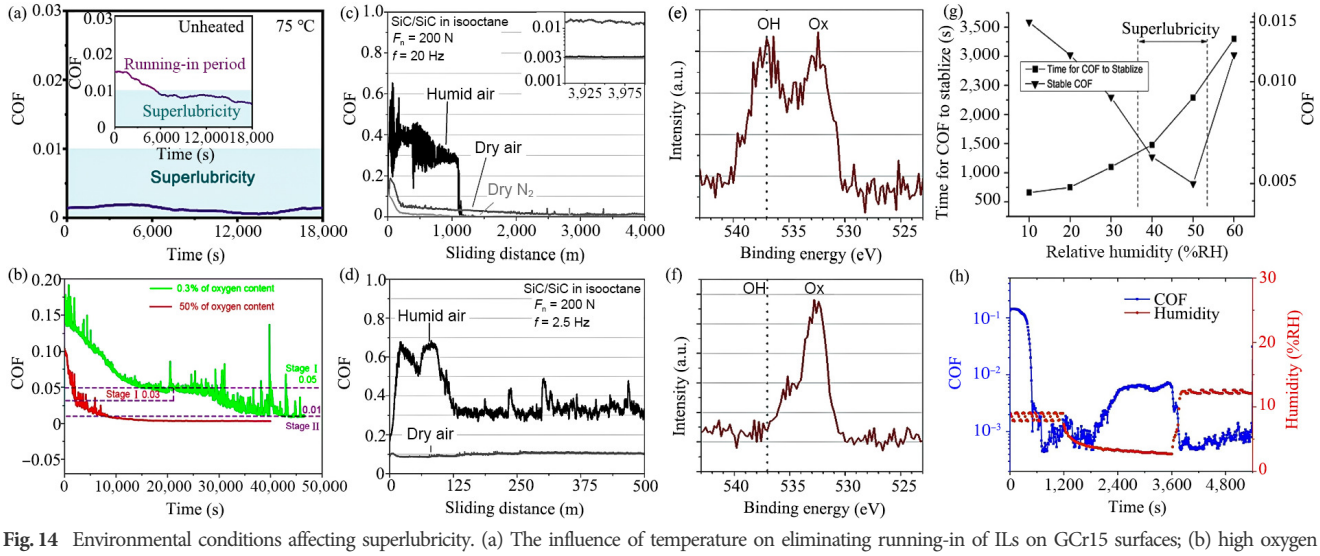

Fig. 14 Environmental conditions affecting superlubricity. (a) The influence of temperature on eliminating running-in of ILs on GCr15 surfaces; (b) high oxygen content shortens the running-in process of DKT solution between GCr15 surfaces; (c–f) the influence of humidity, dry air, and dry N_2 atmosphere on isooctane lubrication between SiC self-mated surfaces, and the XPS results concerning the wear surface tested in humidity and dry air. Influence of humidity on the superlubricity of (g) glycerol solution and (h) glycerol solution mixed with ILs. Reproduced with permission from Ref. [123] for (a), © Elsevier Ltd. 2023; Ref. [121] for (b), © The author(s) 2022; Ref. [152] for (c–f), © Elsevier Ltd. 2019; Ref. [79] for (g, h), © American Chemical Society 2013.

first two requirements. Smooth surfaces not only avoid the mechanical collision of asperities but also enhance the effects of microforces, e.g., hydration forces and hydrodynamic effects. The engineering components have rough surfaces, and a low roughness of less than 50 nm is difficult to fabricate large-scale bearings or curved surfaces, which is one of important reasons limiting the development of liquid superlubricity. Fortunately, with the development of precision manufacturing and surface treatment, components with ultra-low surface roughness are not difficult to process. A low viscosity is needed for liquid lubricants that depend on hydrodynamic effects. The viscosity of liquid lubricants with superlubricity is typically lower than 45 mPa·s or even lower than 15 mPa·s because their superlubricity is commonly obtained via hydrodynamic lubrication (HL). This has been adopted to tailor the superlubricity of neat ILs by dissolving them in water. The low viscosity of aqueous solution accelerates the superlubricity between smooth surfaces that facilitates hydration and hydrodynamic effects, but its thermostability becomes the most concern, e.g., a low boiling point, evaporation of water, and decomposition of unsaturated molecules. The hydration force provides extra support to sustain the normal load even though the aqueous solution might have a low viscosity, but this does not apply to oil-based lubricants. The engineering components are almost entirely lubricated by oil-based liquids that commonly consist of saturated alkanes, e.g., mineral oil, but mineral oil does not appear to have superlubricity properties. An oil-based lubricant with an appreciable load-carrying capacity has high viscosity, which contrasts with the above secondary requirement of achieving superlubricity. The viscosity of oil-based lubricants with superlubricity capacity can reach extremely high levels (e.g., 1,000 mPa·s for silicone oil) [12]. High viscosity provides great load-carrying capacity for oil-based lubricants. Boundary lubrication (BL) avoids the harsh requirement for surface roughness and promotes superlubricity at extremely low velocities. In some situations, the viscosity reduction via decreasing temperature is conducive to achieving superlubricity at boundary lubrication (e.g., oil-based lubrication [105], as shown in Fig. 15), but this does not apply to lubricants that rely on hydrodynamic effects (e.g., aqueous solutions of ILs [123]).

The latest research has focused on identifying superlubricity systems that exhibit appreciable load-carrying properties and extremely short running time. The solid–liquid coupling of superlubricity with 2D materials is a successful method to improve lubrication properties and resolve contact pressure limitations [161, 162], but it should be noted that liquid superlubricity without any solid additives still has many possibilities, but this requires a lot of exploration work and deep-mechanism discovery. Liquid superlubricity has more stringent requirements for the compatibility of liquid molecules and frictional materials. Compared with traditional lubrication, the types of liquid compounds with superlubricity are more limited, and these compounds exhibit strong selectivity for the materials of frictional pairs [163]. Aqueous solutions are more effective for ceramic materials or glass because of their high reactivity with H_2O or hydroxy-containing structures. The load-carrying capacity of the aqueous solution is up to heavy conditions (> 1 GPa), and the hydration force is one of the most significant effects for this high load-carrying capacity, but this key mechanism can hardly be expanded to oil-based superlubricity. Notably, oil-based lubrication is still affected by humidity or H_2O even if the friction pairs are completely immersed in the lubricants and water molecules have extremely low solubility in the oil [164]. Moreover, oil-based liquid lubrication may also release water molecules, especially if the oil-based lubricants contain alcohols or ester additives. Therefore, it is not entirely impossible to introduce hydration forces into oil-based liquid superlubricity. Other mechanisms, such as the hydrodynamic effect and tribological reaction mechanism, have been adapted to non-aqueous lubricants, which would be important directions for breaking through. Oil-based lubricants (e.g., OA, RA, GMO, etc.) exhibit superlubricity, primarily on ta-C coatings with extremely high hardness, and it is invalid for most DLC films with low hardness. Those with unsaturated groups, such as C=C, –OH, and –COOH, are widely expected, and the hydroxyl group seems to play a crucial role in tailoring superlubricity both for aqueous and non-aqueous solutions; however, whether there are other effective chemical groups or molecules that extend the liquid superlubricity mechanism to a wider range of conditions remains elusive. In

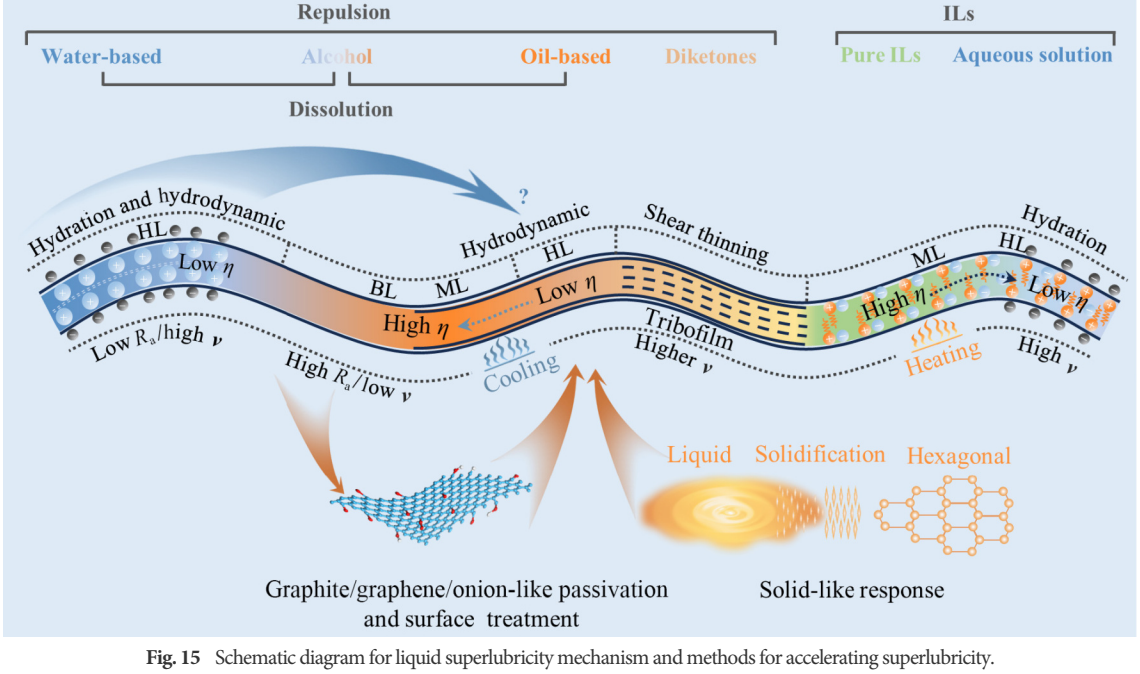

Fig. 15 Schematic diagram for liquid superlubricity mechanism and methods for accelerating superlubricity.

addition, graphite/graphene/onion-like substances play a significant role in achieving the superlubricity of Si_3N_4 self-mated surfaces, Si_3N_4/polycrystalline diamond, Si_3N_4/steel or carbonaceous films, and steel/SiC when lubricated with organic fatty alcohols and fatty acids. Such aromatic passivation mechanism is different from the traditional lubrication theory, which represents an alternative way to realize the superlubricity of oil-based lubricants and even expands the superlubricity of one lubricant to a wider variety of friction materials or the superlubricity of multiple lubricants to one material through surface treatment. The solid-like response of liquids is also another important mechanism to achieve superlubricity, which has been observed at both the micro- and macroscales for lubricants, such as alkanes [165–168], dodecanol [169, 170], and tetracosanol [171]. These lubricants present saturated structures or single reactive site distributions, which are different from those of common superlubricating species. The current approach provides a novel way to achieve superlubricity in saturated or inert liquids; however, the relevant studies mainly rely on molecular dynamic simulations, and there is still a lack of sufficient evidence at the experimental scale.

Furthermore, the long running-in period of liquid superlubricity is still a major challenge, which is usually associated with the limitation of low load-carrying capacity. Severe wear loss is generally induced by both tribochemical reactions and material removal, which is accompanied by a great reduction in contact pressure. The excellent adsorption/film-forming properties and lower corrosion performance of lubricants always seem to be contrary, especially when their superlubricity closely depends on tribological reactions, e.g., DKTs on steel surface and ceramics friction pairs lubricated with aqueous solutions. Thus, the exploration of novel additives and their modifications are important routes for overcoming the limitations of the running-in period. Composite design through multiple additives, such as corrosion inhibitors, dispersing agents and friction modifiers, is a significant method based on the design idea of traditional lubricants, but this is rarely reported in current research. Corrosion inhibitors, which do not affect the superlubricity performance, should be the most basic property. In the case of dispersing agents, the current study of superlubricity predominantly involves micro-quantity lubrication with a lubrication volume of less than 50 μL. Thus, wear debris is typically present at high concentrations; secondary damage cannot be ignored, and particularly that mage is harmful to the realization of superlubricity. The dispersing agent is likely to be considered in future work to weaken the COF fluctuation and shorten the running-in period, which is of great importance for the long-term service of mechanical equipment. Friction modifiers have been used in superlubricity systems, but their performance does not meet expectations. The use of liquid compounds with different functional structures or elements on various friction pairs is still worthwhile and fundamental theoretical and experimental studies are needed. Owing to the lack of depth mechanisms at the molecular scale, researchers cannot theoretically predict whether a compound will have superlubricity properties on the surface a particular material. The dependence of liquid superlubricity on molecular structure is still an open topic, which has pioneering value for developing new superlubricity systems and solving the bottleneck problem of liquid superlubricity.

Acknowledgements

The work is financially supported by the National Natural Science Foundation of China (Nos. 52222506 and 52405203), the Beijing Natural Science Foundation (Nos. 3254033, 3222010 and 3234057), and the China Postdoctoral Science Foundation (Nos. GZB20230341 and 2024M761643).

Declaration of competing interest

The authors have no competing interests to declare that are relevant to the content of this article. The authors Jinjin Li and Xinchun Chen are the Editorial Board Member and Youth Editorial Board Member of this journal, respectively.

References

[1] Ge X Y, Li J J, Luo J B. Macroscale superlubricity achieved with various liquid molecules: A review. *Front Mech Eng* **5**: 2 (2019)

[2] Liu Y Q, Chen L, Liu L, Shi P F, Sun J H, Wang Y, Qian L M. Macroscopic ultra-low friction and wear enabled by carboxylated graphene with glycerol. *Appl Surf Sci* **638**: 158028 (2023)

[3] Wang T, Yang J, Chen S F, Sun Y F, Jia X H, Song H J. Long-term stable superlubricity coatings enabled by the interaction between the polydimethylsiloxane brush and silicone oil. *ACS Appl Mater Inter* **16**(8): 11134–11144 (2024)

[4] Wang C L, Sun J L, Ge C L, Tang H J, Wu P. Synthesis, characterization and lubrication performance of reduced graphene oxide–Al_2O_3 nanofluid for strips cold rolling. *Colloid Surface A* **637**: 128204 (2022)

[5] He J Q, Sun J L, Meng Y N, Yan X D. Preliminary investigations on the tribological performance of hexagonal boron nitride nanofluids as lubricant for steel/steel friction pairs. *Surf Topogr: Metrol Prop* **7**(1): 015022 (2019)

[6] Dong C, Liu Y, Meng Y N, Du S N, Zhu S C, Tian Y, Ma L R. Ion-specific ice provides a facile approach for reducing ice friction. *J Colloid Interf Sci* **675**: 451–460 (2024)

[7] Yang Y F, Zhang R, Dong S W, Ma X Y, Li J J. Macroscopic superlubricity achieved by polyacrylic acid modified Fe_3O_4 nanoparticles as additives. *Tribol Int* **199**: 110045 (2024)

[8] Yu Q Y, Chen X C, Zhang C H, Xu J X, Qi W, Deng W L, Wang Y H, Zhang C X, Tian J S, Li X W. Influencing mechanisms of deposition bias voltage on superlubricious a-C: H films: Key role of nanoclustering structures in controlling structural evolution of transfer film. *Carbon* **196**: 499–509 (2022)

[9] Yu Q Y, Chen X C, Zhang C H, Tian J S, Deng W L, Huang P. Extreme contact pressure-induced *in situ* structural evolution of nanoclusters governing macroscopic superlubricity in a-C:H films. *Carbon* **215**: 118457 (2023)

[10] Tang L Y, Winkeljann B, Feng S F, Song J, Liu Y H. Recent advances in superlubricity of liposomes for biomedical applications. *Colloid Surface B* **218**: 112764 (2022)

[11] Li K, Jiang J M, Amann T, Yuan Y Y, Wang C, Yuan C Q, Neville A. Evaluation of 1,3-diketone as a novel friction modifier for lubricating oils. *Wear* **452**: 203299 (2020)

[12] Li J J, Zhang C H, Deng M M, Luo J B. Superlubricity of silicone oil achieved between two surfaces by running-in with acid solution. *RSC Adv* **5**(39): 30861–30868 (2015)

[13] Tisza L. On the thermal supraconductibility of liquid helium II and the Bose–Einstein statistics. *C R Hebd Seances Acad Sci* **207**: 1035–1037 (1938)

[14] Tomizawa H, Fischer T E. Friction and wear of silicon nitride and silicon carbide in water: Hydrodynamic lubrication at low sliding speed obtained by tribochemical wear. *ASLE Trans* **30**(1): 41–46 (1987)

[15] Hirano M, Shinjo K. Atomistic locking and friction. *Phys Rev B* **41**(17): 11837–11851 (1990)

[16] Raviv U, Tadmor R, Klein J. Shear and frictional interactions between adsorbed polymer layers in a good solvent. *J Phys Chem B* **105**(34): 8125–8134 (2001)

[17] Kano M. Super low friction of DLC applied to engine cam follower lubricated with ester-containing oil. *Tribol Int* **39**(12): 1682–1685 (2006)

[18] Matta C, Joly Pottuz L, De Barros Bouchet M I, Martin J M, Kano

M, Zhang Q, Goddard III W A. Superlubricity and tribochemistry of polyhydric alcohols. *Phys Rev B* **78**: 085436 (2008)
[19] Trunfio-Sfarghiu A M, Berthier Y, Meurisse M H, Rieu J P. Role of nanomechanical properties in the tribological performance of phospholipid biomimetic surfaces. *Langmuir* **24**(16): 8765–8771 (2008)
[20] Li J J, Zhang C H, Luo J B. Superlubricity behavior with phosphoric acid–water network induced by rubbing. *Langmuir* **27**(15): 9413–9417 (2011)
[21] Li H, Wood R J, Rutland M W, Atkin R. An ionic liquid lubricant enables superlubricity to be "switched on" *in situ* using an electrical potential. *Chem Commun* **50**(33): 4368 (2014)
[22] Tang H J, Sun J L, Han Z, Huang Y, Su D X. Molecule structural dependence of tribological and adsorption behaviors of aluminum rolling oil. *Chin J Nonferrous Met* **32**: 2345–2353 (2022) (in Chinese)
[23] Zhou F, Adachi K, Kato K. Sliding friction and wear property of a-C and a-CN_x coatings against SiC balls in water. *Thin Solid Films* **514**(1–2): 231–239 (2006)
[24] Xu J G, Kato K. Formation of tribochemical layer of ceramics sliding in water and its role for low friction. *Wear* **245**(1–2): 61–75 (2000)
[25] He Z Y, Lu J L, Zeng X Q, Shao H Y, Ren T H, Liu W M. Study of the tribological behaviors of S, P-containing triazine derivatives as additives in rapeseed oil. *Wear* **257**(3–4): 389–394 (2004)
[26] Wang X L, Kato K, Adachi K. The lubrication effect of micro-pits on parallel sliding faces of SiC in water. *Tribol Trans* **45**(3): 294–301 (2002)
[27] Wang X L, Kato K, Adachi K, Aizawa K. The effect of laser texturing of SiC surface on the critical load for the transition of water lubrication mode from hydrodynamic to mixed. *Tribol Int* **34**(10): 703–711 (2001)
[28] Zhou Y, Leonard D N, Guo W, Qu J. Understanding tribofilm formation mechanisms in ionic liquid lubrication. *Sci Rep* **7**: 8426 (2017)
[29] Hartung W, Rossi A, Lee S, Spencer N D. Aqueous Lubrication of SiC and Si_3N_4 ceramics aided by a brush-like copolymer additive, poly(l-lysine)-graft-poly(ethylene glycol). *Tribol Lett* **34**(3): 201–210 (2009)
[30] Duan Y Q, Liu Y H, Zhang C X, Chen Z, Wen S Z. Insight into the tribological behavior of liposomes in artificial joints. *Langmuir* **32**(42): 10957–10966 (2016)
[31] Gao Y, Ma L R, Liang Y, Li B H, Luo J B. Water molecules on the liquid superlubricity interfaces achieved by phosphoric acid solution. *Biosurf Biotribol* **4**(3): 94–98 (2018)
[32] Ge X Y, Li J J, Zhang C H, Luo J B. Liquid superlubricity of polyethylene glycol aqueous solution achieved with boric acid additive. *Langmuir* **34**(12): 3578–3587 (2018)
[33] Gao Y, Ma L R, Luo J B. Pitted surfaces produced by lactic acid lubrication and their effect on ultra-low friction. *Tribol Lett* **57**(2): 20 (2015)
[34] Li J J, Zhang C H, Sun L, Lu X C, Luo J B. Tribochemistry and superlubricity induced by hydrogen ions. *Langmuir* **28**(45): 15816–15823 (2012)
[35] Li J J, Zhang C H, Luo J B. Superlubricity achieved with mixtures of polyhydroxy alcohols and acids. *Langmuir* **29**(17): 5239–5245 (2013)
[36] Zhang C H, Ma Z Z, Luo J B, Lu X C, Wen S Z. Superlubricity of a mixed aqueous solution. *Chin Phys Lett* **28**(5): 056201 (2011)
[37] Li J J, Zhang C H, Ma L R, Liu Y H, Luo J B. Superlubricity achieved with mixtures of acids and glycerol. *Langmuir* **29**(1): 271–275 (2013)
[38] Carrión F J, Martínez-Nicolás G, Iglesias P, Sanes J, Bermúdez M D. Liquid crystals in tribology. *Int J Mol Sci* **10**(9): 4102–4115 (2009)
[39] Eidenschink R. Liquid crystals in variable friction devices. *Angew Chem Int Ed* **27**(11): 1579–1580 (1988)
[40] Walter M, Amann T, Li K, Kailer A, Rühe J, Moseler M. 1,3-Diketone fluids and their complexes with iron. *J Phys Chem A* **117**(16): 3369–3376 (2013)
[41] Amann T, Kailer A. Ultralow friction of mesogenic fluid mixtures in tribological reciprocating systems. *Tribol Lett* **37**(2): 343–352 (2010)
[42] Amann T, Kailer A. Relationship between ultralow friction of mesogenic-like fluids and their lateral chain length. *Tribol Lett* **41**(1): 121–129 (2011)
[43] Amann T, Kailer A. Analysis of the ultralow friction behavior of a mesogenic fluid in a reciprocating contact. *Wear* **271**(9–10): 1701–1706 (2011)
[44] Zhou Y, Qu J. Ionic liquids as lubricant additives: A review. *ACS Appl Mater Inter* **9**(4): 3209–3222 (2017)
[45] Liang H Y, Yin T Q, Liu M Q, Fu C H, Xia X J, Zou S J, Hua X J, Fu Y H, Bu Y F. Unravelling high-load superlubricity of ionic liquid analogues by *in situ* Raman: Incomplete hydration induced by competitive exchange of external water with crystalline water. *J Phys Chem Lett* **14**(2): 453–459 (2023)
[46] Liang H Y, Xia X J, Liu M Q, Zou S J, Yin T Q, Li H F, Zhang Y H, Min C Y, Bu Y F. Competition-induced macroscopic superlubricity of ionic liquid analogues by hydroxyl ligands revealed by *in situ* Raman. *Langmuir* **40**(8): 4277–4284 (2024)
[47] Zheng Z W, Chen H J, Xu Y K, Liu X L, Wang H Z, Meng W S, Feng D P, Qiao D. Effective superlubricity behavior triggered by interfacial tribochemical reactions from simple protic ionic liquids aqueous. *Chem Eng J* **485**: 149465 (2024)
[48] Espinosa T, Jiménez M, Sanes J, Jiménez A E, Iglesias M, Bermúdez M D. Ultra-low friction with a protic ionic liquid boundary film at the water-lubricated sapphire–stainless steel interface. *Tribol Lett* **53**(1): 1–9 (2014)
[49] Ye C F, Liu W M, Chen Y X, Yu L G. Room-temperature ionic liquids: A novel versatile lubricant. *Chem Commun* **21**: 2244–2245 (2001)
[50] Wang Z N, Li J J, Liu Y H, Luo J B. Macroscale superlubricity achieved between zwitterionic copolymer hydrogel and sapphire in water. *Mater Des* **188**: 108441 (2020)
[51] Raviv U, Giasson S, Kampf N, Gohy J F, Jérôme R, Klein J. Lubrication by charged polymers. *Nature* **425**(6954): 163–165 (2003)
[52] Chen M, Briscoe W H, Armes S P, Cohen H, Klein J. Polyzwitterionic brushes: Extreme lubrication by design. *Eur Polym J* **47**(4): 511–523 (2011)
[53] Chen M, Briscoe W H, Armes S P, Klein J. Lubrication at physiological pressures by polyzwitterionic brushes. *Science* **323**(5922): 1698–1701 (2009)
[54] Kampf N, Gohy J F, Jérôme R, Klein J. Normal and shear forces between a polyelectrolyte brush and a solid surface. *J Polym Sci Polym Phys* **43**(2): 193–204 (2005)
[55] Adibnia V, Olszewski M, De Crescenzo G, Matyjaszewski K, Banquy X. Superlubricity of zwitterionic bottlebrush polymers in the presence of multivalent ions. *J Am Chem Soc* **142**(35): 14843–14847 (2020)
[56] Beheshti A, Huang Y, Blakey I, Stokes J R. Macroscale superlubricity induced by film-forming polymer brush-grafted colloidal additives. *J Colloid Interf Sci* **634**: 703–714 (2023)
[57] Vlădescu S C, Tadokoro C, Miyazaki M, Reddyhoff T, Nagamine T, Nakano K, Sasaki S, Tsujii Y. Exploiting the synergy between concentrated polymer brushes and laser surface texturing to achieve durable superlubricity. *ACS Appl Mater Inter* **14**(13): 15818–15829 (2022)
[58] Xiao Y Y, Shi W K, Luo J, Liao Y J. The tribological performance of TiN, WC/C and DLC coatings measured by the four-ball test. *Ceram Int* **40**(5): 6919–6925 (2014)
[59] Du C H, Yu T T, Zhang L Q, Shen R L, Wu Z S, Li X J, He X J, Feng Y G, Wang D A. Robust and universal macroscale superlubricity with natural phytic acid solutions. *Tribol Int* **183**: 108387 (2023)
[60] Goldberg R, Schroeder A, Silbert G, Turjeman K, Barenholz Y, Klein J. Boundary lubricants with exceptionally low friction coefficients based on 2D close-packed phosphatidylcholine liposomes. *Adv Mater* **23**(31): 3517–3521 (2011)
[61] Goldberg R, Schroeder A, Barenholz Y, Klein J. Interactions between adsorbed hydrogenated soy phosphatidylcholine (HSPC)

vesicles at physiologically high pressures and salt concentrations. *Biophys J* **100**(10): 2403–2411 (2011)
[62] Gaisinskaya-Kipnis A, Klein J. Normal and frictional interactions between liposome-bearing biomacromolecular bilayers. *Biomacromolecules* **17**(8): 2591–2602 (2016)
[63] Raj A, Wang M, Zander T, Florian Wieland D C, Liu X Y, An J X, Garamus V M, Willumeit-Römer R, Fielden M, Claesson P M, et al. Lubrication synergy: Mixture of hyaluronan and dipalmitoylphosphatidylcholine (DPPC) vesicles. *J Colloid Interf Sci* **488**: 225–233 (2017)
[64] Li J J, Cao W, Wang Z N, Ma M, Luo J B. Origin of hydration lubrication of zwitterions on graphene. *Nanoscale* **10**(35): 16887–16894 (2018)
[65] Duan Y Q, Liu Y H, Li J J, Feng S F, Wen S Z. AFM study on superlubricity between Ti_6Al_4V/polymer surfaces achieved with liposomes. *Biomacromolecules* **20**(4): 1522–1529 (2019)
[66] Sheng D Z, Zhou J X, Zhang H D, Tian H T, Liu X C, Qi X L, Zhang H C, Wang W W. Achievement of super-low friction between ultra-polished quartz lubricated by hydrated hydroxyethyl cellulose. *J Mater Eng Perform* **31**(2): 1096–1107 (2022)
[67] Li J J, Zhang C H, Cheng P, Chen X C, Wang W Q, Luo J B. AFM studies on liquid superlubricity between silica surfaces achieved with surfactant micelles. *Langmuir* **32**(22): 5593–5599 (2016)
[68] Wen X L, Bai P P, Li Y Z, Cao H, Li S W, Wang B, Fang J B, Meng Y G, Ma L R, Tian Y. Effects of abrasive particles on liquid superlubricity and mechanisms for their removal. *Langmuir* **37**(12): 3628–3636 (2021)
[69] Li S W, Bai P P, Li Y Z, Jia W P, Li X X, Meng Y G, Ma L R, Tian Y. Extreme-pressure superlubricity of polymer solution enhanced with hydrated salt ions. *Langmuir* **36**(24): 6765–6774 (2020)
[70] Han T Y, Zhang C H, Luo J B. Macroscale superlubricity enabled by hydrated alkali metal ions. *Langmuir* **34**(38): 11281–11291 (2018)
[71] Han T Y, Zhang C H, Li J J, Yuan S H, Chen X C, Zhang J Y, Luo J B. Origins of superlubricity promoted by hydrated multivalent ions. *J Phys Chem Lett* **11**(1): 184–190 (2020)
[72] Nagabhooshanam N, Baskar S, Prabhu T R, Arumugam S. Evaluation of tribological characteristics of nano zirconia dispersed biodegradable canola oil methyl ester metalworking fluid. *Tribol Int* **151**: 106510 (2020)
[73] Liu W R, Wang H D, Liu Y H, Li J J, Erdemir A, Luo J B. Mechanism of superlubricity conversion with polyalkylene glycol aqueous solutions. *Langmuir* **35**(36): 11784–11790 (2019)
[74] Wang H D, Liu Y H, Liu W R, Liu Y M, Wang K P, Li J J, Ma T B, Eryilmaz O L, Shi Y J, Erdemir A, et al. Superlubricity of polyalkylene glycol aqueous solutions enabled by ultrathin layered double hydroxide nanosheets. *ACS Appl Mater Inter* **11**(22): 20249–20256 (2019)
[75] Wang H D, Liu Y H, Li J J, Luo J B. Investigation of superlubricity achieved by polyalkylene glycol aqueous solutions. *Adv Mater Interfaces* **3**(19): 1600531 (2016)
[76] Jia W P, Bai P P, Zhang W L, Ma L R, Meng Y G, Tian Y. On lubrication states after a running-in process in aqueous lubrication. *Langmuir* **35**: 15435–15443 (2019)
[77] Liu P X, Liu Y H, Yang Y, Chen Z, Li J J, Luo J B. Mechanism of biological liquid superlubricity of *Brasenia schreberi* mucilage. *Langmuir* **30**(13): 3811–3816 (2014)
[78] Zhang L, Liu Y H, Chen Z, Liu P X. Behavior and mechanism of ultralow friction of basil seed gel. *Colloid Surface A* **489**: 454–460 (2016)
[79] Chen Z, Liu Y H, Zhang S H, Luo J B. Controllable superlubricity of glycerol solution *via* environment humidity. *Langmuir* **29**(38): 11924–11930 (2013)
[80] Li J J, Zhang C H, Deng M M, Luo J B. Investigation of the difference in liquid superlubricity between water- and oil-based lubricants. *RSC Adv* **5**(78): 63827–63833 (2015)
[81] Zhou X X, Lin B, Yan S, Wang A Y, Zhang X F, Ge S D. Influence of temperature and concentration on tribological properties of silicon nitride in glycerol aqueous solution. *Ceram Int* **42**(3): 3786–3796 (2016)
[82] Han K, Ma P S, Ma L R, Tian Y, Luo J B. Investigation of the running-in process in photoinduced superlubricity. *Front Mater* **10**: 1109890 (2023)
[83] Sun S Y, Yi S, Li J J, Ding Z M, Song W, Luo J B. Lithium citrate triggered macroscopic superlubricity with near-zero wear on an amorphous carbon film. *ACS Appl Mater Inter* **15**(15): 19705–19714 (2023)
[84] Liu W R, Wang H D, Liu Y H. Adjustable superlubricity system using polyalkylene glycol with various acid aqueous solutions. *Friction* **11**(7): 1138–1149 (2023)
[85] Ge X Y, Halmans T, Li J J, Luo J B. Molecular behaviors in thin film lubrication: Part three: Superlubricity attained by polar and nonpolar molecules. *Friction* **7**(6): 625–636 (2019)
[86] Björling M, Shi Y J. DLC and glycerol: Superlubricity in rolling/sliding elastohydrodynamic lubrication. *Tribol Lett* **67**(1): 23 (2019)
[87] Long Y, De Barros Bouchet M I, Lubrecht T, Onodera T, Martin J M. Superlubricity of glycerol by self-sustained chemical polishing. *Sci Rep* **9**: 6286 (2019)
[88] Liu Y F, Li J J, Ge X Y, Yi S, Wang H D, Liu Y H, Luo J B. Macroscale superlubricity achieved on the hydrophobic graphene coating with glycerol. *ACS Appl Mater Inter* **12**(16): 18859–18869 (2020)
[89] Long Y, Kuwahara T, De Barros Bouchet M I, Ristić A, Dörr N, Lubrecht T, Dupuy L, Moras G, Martin J M, Moseler M. *In situ* synthesis of graphene nitride nanolayers on glycerol-lubricated Si_3N_4 for superlubricity applications. *ACS Appl Nano Mater* **4**(3): 2721–2732 (2021)
[90] Ma Q, Wang W, Dong G N. Achieving macroscale liquid superlubricity using lubricant mixtures of glycerol and propanediol. *Tribol Lett* **69**(4): 159 (2021)
[91] Liu M M, Wang L H, Zhang C X, Cheng Y H, Yang C B, Liu Z F. Regulation mechanism for friction coefficient of poly (vinylphosphoric acid) (PVPA) superlubricity system based on ionic properties. *Nanomaterials* **12**(13): 2308 (2022)
[92] Sun S Y, Li J F, Li J J, Luo J B. Enhanced superlubricity on a-C films by lubrication with 3-hydroxypropionic acid. *Carbon* **199**: 161–169 (2022)
[93] Li Y L, Sha X H, Yue W, Qin W B, Wang C B. Effects of tribochemical reaction on tribological behaviors of Si_3N_4/polycrystalline diamond in hydrochloric acid. *Int J Refract Met H* **79**: 197–203 (2019)
[94] Jiang Y Y, Xiao C, Chen L, Li J J, Zhang C H, Zhou N N, Qian L M, Luo J B. Temporary or permanent liquid superlubricity failure depending on shear-induced evolution of surface topography. *Tribol Int* **161**: 107076 (2021)
[95] Deng M M, Zhang C H, Li J J, Ma L R, Luo J B. Hydrodynamic effect on the superlubricity of phosphoric acid between ceramic and sapphire. *Friction* **2**(2): 173–181 (2014)
[96] Li J J, Ma L R, Zhang S H, Zhang C H, Liu Y H, Luo J B. Investigations on the mechanism of superlubricity achieved with phosphoric acid solution by direct observation. *J Appl Phys* **114**(11): 114901 (2013)
[97] Sun L, Zhang C H, Li J J, Liu Y H, Luo J B. Superlubricity of Si_3N_4 sliding against SiO_2 under linear contact conditions in phosphoric acid solutions. *Sci China Technol Sci* **56**(7): 1678–1684 (2013)
[98] Li J J, Zhang C H, Luo J B. Effect of pH on the liquid superlubricity between Si_3N_4 and glass achieved with phosphoric acid. *RSC Adv* **4**(86): 45735–45741 (2014)
[99] Xiao C, Li J J, Chen L, Zhang C H, Zhou N N, Qian L M, Luo J B. Speed dependence of liquid superlubricity stability with H_3PO_4 solution. *RSC Adv* **7**(78): 49337–49343 (2017)
[100] Xiao C, Li J J, Chen L, Zhang C H, Zhou N N, Qing T, Qian L M, Zhang J Y, Luo J B. Water-based superlubricity in vacuum. *Friction* **7**(2): 192–198 (2019)
[101] Li J J, Zhang C H, Deng M M, Luo J B. Investigations of the superlubricity of sapphire against ruby under phosphoric acid lubrication. *Friction* **2**(2): 164–172 (2014)
[102] Du C H, Yu T T, Wu Z S, Zhang L Q, Shen R L, Li X J, Feng M,

Feng Y G, Wang D A. Achieving macroscale superlubricity with ultra-short running-in period by using polyethylene glycol-tannic acid complex green lubricant. *Friction* **11**(5): 748–762 (2023)
[103] Li J J, Zhang C H, Deng M M, Luo J B. Reduction of friction stress of ethylene glycol by attached hydrogen ions. *Sci Rep* **4**: 7226 (2014)
[104] Wen X L, Bai P P, Meng Y G, Ma L R, Tian Y. High-temperature superlubricity realized with chlorinated-phenyl and methyl-terminated silicone oil and hydrogen-ion running-in. *Langmuir* **38** (32): 10043–10051 (2022)
[105] Long Y, Martin J M, Dubreuil F, De Barros Bouchet M I. Achieving superlubricity of ricinoleic acid in the steel/Si_3N_4 contact under boundary lubrication. *Tribol Lett* **70**(4): 109 (2022)
[106] Pan J J, Gao X X, Liu C, Zhang K, Zheng W T, Chen C F. Macroscale superdurable superlubricity achieved in lubricant oil via operando tribochemical formation of fullerene-like carbon. *Cell Rep* **3**(11): 101130 (2022)
[107] Li K, Amann T, List M, Walter M, Moseler M, Kailer A, Rühe J. Ultralow friction of steel surfaces using a 1,3-diketone lubricant in the thin film lubrication regime. *Langmuir* **31**(40): 11033–11039 (2015)
[108] Kuwahara T, Romero P A, Makowski S, Weihnacht V, Moras G, Moseler M. Mechano-chemical decomposition of organic friction modifiers with multiple reactive centres induces superlubricity of ta-C. *Nat Commun* **10**: 151 (2019)
[109] De Barros Bouchet M I, Martin J M, Avila J, Kano M, Yoshida K, Tsuruda T, Bai S D, Higuchi Y, Ozawa N, Kubo M, et al. Diamond-like carbon coating under oleic acid lubrication: Evidence for graphene oxide formation in superlow friction. *Sci Rep* **7**: 46394 (2017)
[110] Long Y, Wang Y, Weihnacht V, Makowski S, Kubo M, Martin J M, De Barros Bouchet M I. Mechanism of superlubricity of a DLC/Si_3N_4 contact in the presence of castor oil and other green lubricants. *Friction* **10**(10): 1693–1706 (2022)
[111] Long Y, Galipaud J, Weihnacht V, Makowski S, Martin J M, De Barros Bouchet M I. Achieving superlubricity using selected tribo-pairs lubricated by castor oil and unsaturated fatty acids. *Tribol Int* **169**: 107462 (2022)
[112] Zeng Q F, Dong G N. Influence of load and sliding speed on super-low friction of nitinol 60 alloy under castor oil lubrication. *Tribol Lett* **52**(1): 47–55 (2013)
[113] Zeng Q F, Dong G N. Superlubricity behaviors of Nitinol 60 alloy under oil lubrication. *T Nonferr Metal Soc* **24**(2): 354–359 (2014)
[114] Li K, Amann T, Walter M, Moseler M, Kailer A, Rühe J. Ultralow friction induced by tribochemical reactions: A novel mechanism of lubrication on steel surfaces. *Langmuir* **29**(17): 5207–5213 (2013)
[115] Li J Y, Yuan Y Y, Amann T, Yuan C Q, Li K. Macroscopic oil-based superlubricity achieved on steel surfaces with the roughness of engineering level. *Tribol Lett* **71**(2): 32 (2023)
[116] Liu D S, Li K, Zhang S M, Amann T, Zhang C H, Yan X P. Anti-spreading behavior of 1,3-diketone lubricating oil on steel surfaces. *Tribol Int* **121**: 108–113 (2018)
[117] Li K, Zhang S M, Liu D S, Amann T, Zhang C H, Yuan C Q, Luo J B. Superlubricity of 1,3-diketone based on autonomous viscosity control at various velocities. *Tribol Int* **126**: 127–132 (2018)
[118] Zhang S M, Zhang C H, Chen X C, Li K, Jiang J M, Yuan C Q, Luo J B. XPS and ToF-SIMS analysis of the tribochemical absorbed films on steel surfaces lubricated with diketone. *Tribol Int* **130**: 184–190 (2019)
[119] Du S N, Zhang C H, Luo Z. The synergistic effect of diketone and its chelate enables macroscale superlubricity for a steel/steel contact. *Tribol Int* **173**: 107610 (2022)
[120] Yuan Y Y, Amann T, Xu Y W, Zhang Y, Chen J F, Yuan C Q, Li K. Load and velocity boundaries of oil-based superlubricity using 1,3-diketone. *Friction* **11**(5): 704–715 (2023)
[121] Jiang Y Y, Chen L, Xiao C, Zhang S M, Zhang C H, Zhou N N, Qin T, Qian L M, Zhang J Y. How to improve superlubricity performance of diketone at steel interface: Effects of oxygen gas. *Friction* **11**(6): 927–937 (2023)
[122] Zhang S M, Zhang C H, Li K, Luo J B. Investigation of ultra-low friction on steel surfaces with diketone lubricants. *RSC Adv* **8**(17): 9402–9408 (2018)
[123] Chen H Y, Cai T, Li H, Ruan X X, Jiao C C, Atkin R, Wang Y D, Gong P, Zhou X Y, Yu J H, et al. Macroscale superlubricity of steel by polymer-based ionic liquids without a running-in period. *Tribol Int* **182**: 108349 (2023)
[124] Zheng Q K, Chhattal M, Bai C N, Zheng Z W, Qiao D, Gong Z B, Zhang J Y. Superlubricity of PTFE triggered by green ionic liquids. *Appl Surf Sci* **614**: 156241 (2023)
[125] Wang K, Liu L, Liu Y, Luo J. Simple but effective: Liquid superlubricity with high load capacity achieved by ionic liquids. *Mater Today Nano* **20**: 100257 (2022)
[126] Ge X Y, Li J J, Zhang C H, Liu Y H, Luo J B. Superlubricity and antiwear properties of in situ-formed ionic liquids at ceramic interfaces induced by tribochemical reactions. *ACS Appl Mater Inter* **11**(6): 6568–6574 (2019)
[127] Ge X Y, Li J J, Zhang C H, Wang Z N, Luo J B. Superlubricity of 1-ethyl-3-methylimidazolium trifluoromethanesulfonate ionic liquid induced by tribochemical reactions. *Langmuir* **34**(18): 5245–5252 (2018)
[128] Arafune H, Kamijo T, Morinaga T, Honma S, Sato T, Tsujii Y. A robust lubrication system using an ionic liquid polymer brush. *Adv Mater Interfaces* **2**(15): 1500187 (2015)
[129] Han T Y, Zhao M B, Sun C, Zhao R Q, Xu W X, Zhang S M, Singh S, Luo J B, Zhang C H. Macroscale superlubricity of hydrated anions in the boundary lubrication regime. *ACS Appl Mater Inter* **15**(35): 42094–42103 (2023)
[130] Al Kaisy G M J, Mutalib M I A, Rao T V V L N, Senatore A. Tribological performance of low viscosity halogen-free ammonium based protic ionic liquids with carboxylate anions as neat lubricants. *Tribol Int* **160**: 107058 (2021)
[131] Zheng Z W, Liu X L, Yu H X, Chen H J, Feng D P, Qiao D. Insight into macroscale superlubricity of polyol aqueous solution induced by protic ionic liquid. *Friction* **10**(12): 2000–2017 (2022)
[132] Li X W, Zhang D K, Xu X W, Lee K R. Tailoring the nanostructure of graphene as an oil-based additive: Toward synergistic lubrication with an amorphous carbon film. *ACS Appl Mater Inter* **12**(38): 43320–43330 (2020)
[133] Zheng Z W, Liu X L, Huang G W, Chen H J, Yu H X, Feng D P, Qiao D. Macroscale superlubricity achieved via hydroxylated hexagonal boron nitride nanosheets with ionic liquid at steel/steel interface. *Friction* **10**(9): 1365–1381 (2022)
[134] Li J F, Li J J. Synergistic lubrication effect between oxidized black phosphorus and oil molecules triggers superlubricity. *J Phys Chem Lett* **13**(35): 8245–8253 (2022)
[135] Tang G B, Wu Z B, Su F H, Wang H D, Xu X, Li Q, Ma G Z, Chu P K. Macroscale superlubricity on engineering steel in the presence of black phosphorus. *Nano Lett* **21**(12): 5308–5315 (2021)
[136] Ge X Y, Li J J, Wang H D, Zhang C H, Liu Y H, Luo J B. Macroscale superlubricity under extreme pressure enabled by the combination of graphene-oxide nanosheets with ionic liquid. *Carbon* **151**: 76–83 (2019)
[137] Klein J. Hydration lubrication. *Friction* **1**(1): 1 (2013)
[138] Müller M, Lee S, Spikes H A, Spencer N D. The influence of molecular architecture on the macroscopic lubrication properties of the brush-like co-polyelectrolyte poly(L-lysine)-g-poly(ethylene glycol) (PLL-g-PEG) adsorbed on oxide surfaces. *Tribol Lett* **15**(4): 395–405 (2003)
[139] Han T Y, Zhang S W, Zhang C H. Unlocking the secrets behind liquid superlubricity: A state-of-the-art review on phenomena and mechanisms. *Friction* **10**(8): 1137–1165 (2022)
[140] Wang W, Xie G X, Luo J B. Superlubricity of black phosphorus as

lubricant additive. *ACS Appl Mater Inter* **10**(49): 43203–43210 (2018)
[141] Han T Y, Yi S, Zhang C H, Li J J, Chen X C, Luo J B, Banquy X. Superlubrication obtained with mixtures of hydrated ions and polyethylene glycol solutions in the mixed and hydrodynamic lubrication regimes. *J Colloid Interf Sci* **579**: 479–488 (2020)
[142] Jia W P, Tian J M, Bai P P, Li S W, Zeng H B, Zhang W L, Tian Y. A novel comb-typed poly(oligo(ethylene glycol) methylether acrylate) as an excellent aqueous lubricant. *J Colloid Interf Sci* **539**: 342–350 (2019)
[143] Amann T, Kailer A, Oberle N, Li K, Walter M, List M, Rühe J. Macroscopic superlow friction of steel and diamond-like carbon lubricated with a formanisotropic 1,3-diketone. *ACS Omega* **2**(11): 8330–8342 (2017)
[144] Yang J W, Yuan Y Y, Li K, Amann T, Wang C, Yuan C Q, Neville A. Ultralow friction of 5CB liquid crystal on steel surfaces using a 1,3-diketone additive. *Wear* **480**: 203934 (2021)
[145] Du S N, Zhang C H, Luo Z. Combination of diketone and PAO to achieve macroscale oil-based superlubricity at relative high contact pressures. *Friction* **12**(5): 869–883 (2024)
[146] Du S N, Zhang C H, Luo Z. Effect of the molecular structure of 1, 3-diketones on the realization of oil-based superlubricity on steel/steel friction pairs. *Langmuir* **40**(1): 805–817 (2024)
[147] Dhanola A, Khanna N, Gajrani K K. A critical review on liquid superlubricitive technology for attaining ultra-low friction. *Renew Sust Energ Rev* **165**: 112626 (2022)
[148] Han T Y, Cao W, Xu Z, Adibnia V, Olgiati M, Valtiner M, Ma L R, Zhang C H, Ma M, Luo J B. Hydration layer structure modulates superlubrication by trivalent La^{3+} electrolytes. *Sci Adv* **9**(28): eadf3902 (2023)
[149] Zhang S W, Zhang C H, Hu Y Z, Ma L R. Numerical simulation of mixed lubrication considering surface forces. *Tribol Int* **140**: 105878 (2019)
[150] Chen Z, Liu Y H, Luo J B. Superlubricity of nanodiamonds glycerol colloidal solution between steel surfaces. *Colloid Surface A* **489**: 400–406 (2016)
[151] Hua J, Björling M, Larsson R, Shi Y J. Controllable superlubricity achieved with mixtures of green ionic liquid and glycerol aqueous solution via humidity. *J Mol Liq* **345**: 117860 (2022)
[152] Schreiber P J, Schneider J. Liquid superlubricity obtained for self-mated silicon carbide in nonaqueous low-viscosity fluid. *Tribol Int* **134**: 7–14 (2019)
[153] Smallwood I M. *Handbook of Organic Solvent Properties*. Oxford (UK): Elsevier, 1996.
[154] Vigil G, Xu Z H, Steinberg S, Israelachvili J. Interactions of silica surfaces. *J Colloid Interf Sci* **165**(2): 367–385 (1994)
[155] Iler R. *The Chemistry of Silica: Solubility, Polymerization, Colloid and Surface Properties and Biochemistry of Silica*. New York (USA): Wiley, 1980.
[156] Hofmann S, Lohner T,Stahl K. Influence of water evaporation on elastohydrodynamic lubrication with water-containing polyalkylene glycols. *Friction* **12**(10): 2370–2388 (2024)
[157] Ma Q, Yan C P, Yan R, Xu X, Wang H F. Towards direct superlubricity and superlow wear via amino modification of polyhydroxy alcohol solutions. *Friction* **12**(9): 1980–1990 (2024)
[158] Wang H D, Wu J, Wang K P, Su Y J, Zhang X C, Liu Y H, Zhang J H. Simple and effective: Superlubricity behaviour of the G-quadruplex hydrogel with high selectivity for K^+ ions based on the ocular environment. *Friction* **12**: 2548–2562 (2024)
[159] Baykara M Z, Vazirisereshk M R, Martini A. Emerging superlubricity: A review of the state of the art and perspectives on future research. *Appl Phys Rev* **5**(4): 041102 (2018)
[160] Zhang X Q, Fan J Y, Cui Z C, Cao T F, Shi J Q, Zhou F, Liu W M, Fan X L. Structural superlubricity at homogenous interface of penta-graphene. *Friction* **12**: 2004–2017 (2024)
[161] Wu S, Gu J, Li R T, Tang Y N, Gao L X, An C H, Deng Q B, Zhao L B, Hu N. Progress on mechanical and tribological characterization of 2D materials by AFM force spectroscopy. *Friction* **12**: 2627–2656 (2024)
[162] Jiang Z Q, Sun Y K, Liu B K, Yu L G, Tong Y P, Yan M M, Yang Z Z, Hao Y X, Shangguan L J, Zhang S M, et al. Research progresses of nanomaterials as lubricant additives. *Friction* **12**(7): 1347–1391 (2024)
[163] Zhong C L, Hu K H, Xu Y, Hu E Z, Hu X G. Lubrication antagonism mechanism of nano-MoS_2 and soot particles in ester base oil. *Friction* **12**: 2692–2706 (2024)
[164] Yi X B, Xu H Y, Jin G, Lu Y, Chen B Q, Xu S F, Shi J Q, Fan X L. Boundary slip and lubrication mechanisms of organic friction modifiers with effect of surface moisture. *Friction* **12**: 1483–1498 (2024)
[165] Jabbarzadeh A, Harrowell P, Tanner R I. Very low friction state of a dodecane film confined between mica surfaces. *Phys Rev Lett* **94**(12): 126103 (2005)
[166] Gao J P, Luedtke W D, Landman U. Structure and solvation forces in confined films: Linear and branched alkanes. *J Chem Phys* **106** (10): 4309–4318 (1997)
[167] Zhu Y X, Granick S. Superlubricity: A paradox about confined fluids resolved. *Phys Rev Lett* **93**(9): 096101 (2004)
[168] Smith A M, Hallett J E, Perkin S. Solidification and superlubricity with molecular alkane films. *P Natl Acad Sci USA* **116**(51): 25418–25423 (2019)
[169] Wang P, Reddyhoff T. Wall slip in an EHL contact lubricated with 1-dodecanol. *Tribol Int* **113**: 197–205 (2017)
[170] Reddyhoff T, Ewen J P, Deshpande P, Frogley M D, Welch M D, Montgomery W. Macroscale superlubricity and polymorphism of long-chain *n*-alcohols. *ACS Appl Mater Inter* **13**(7): 9239–9251 (2021)
[171] Yagi K, Vergne P. Abnormal film shapes in sliding elastohydrodynamic contacts lubricated by fatty alcohols. *P I Mech Eng E—J Pro* **221**(3): 287–300 (2007)

Huajie Tang received his B.S. degree in 2017 and his Ph.D. degree in 2023, both in materials science and engineering from the University of Science and Technology Beijing, China. From December 2021 to August 2022, he served as a visiting scholar at the KTH Royal Institute of Technology in Sweden. He is currently a postdoctoral researcher at the State Key Laboratory of Tribology, Tsinghua University, China. His research interests include carbon film technology, liquid superlubricity, engineering lubrication, and metal corrosion.

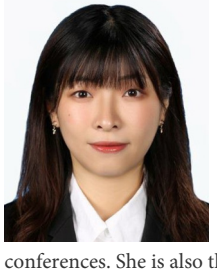

Wenli Deng received her Ph.D. degree in mechanical engineering from the University of Science and Technology of Beijing, China, in 2020. She is currently an assistant professor at Tsinghua University, China. Her major research areas include friction, superlubricity, and interface science. She has published more than 25 SCI papers with an h-index of 18. She has authorized 5 invention patents and has given more than 5 invited speeches at academic conferences. She is also the author of 3 professional books.

Jinjin Li received his B.S. degree in mechanical engineering from the University of Science and Technology of China in 2009 and his Ph.D. degree in mechanical engineering from Tsinghua University, China, in 2014. He is currently a tenured associate professor at Tsinghua University. His major research areas include friction, superlubricity, and interface science. He has published more than 100 papers indexed by SCI with more than 5,000 citations

and an h-index of 45. He has authorized 20 invention patents and has given more than 10 keynote/invited speeches at academic conferences.

Jiaqi He received his Ph.D. degree in 2022 in materials science and engineering from the University of Science and Technology Beijing, China. He is currently a lecturer at the Open University of China. His research interests include the friction and lubrication of metal-working processes, and molecular dynamics simulations and machine learning prediction of tribological behaviors.

Xinchun Chen received his Ph.D. degree in mechanical engineering in 2014 from The University of Tokyo, Japan. He subsequently joined the SKLT at Tsinghua University, China. His current position is an associate professor of the SKLT. His research areas cover coating technology, the tribology of solid lubricants, nanomaterials, superlubricity, and surface and interface phenomena. He has published more than 90 papers indexed by SCI. He has authorized 20 invention patents and delivered more than 20 keynote/invited talks at academic conferences.